Article

Novel Sigma Receptors Ligands-Nitric Oxide Photodonor: Molecular Hybrids for Double-Targeted Antiproliferative Effect

Emanuele Amata, Maria Dichiara, Emanuela Arena, Valeria Pittalà, Venerando Pistarà, Venera Cardile, Adriana Carol Eleonora Graziano, Aurore Fraix, Agostino Marrazzo, Salvatore Sortino, and Orazio Prezzavento

J. Med. Chem., **Just Accepted Manuscript** • DOI: 10.1021/acs.jmedchem.7b00791 • Publication Date (Web): 27 Nov 2017

Novel Sigma Receptors Ligands-Nitric Oxide Photodonor: Molecular Hybrids for Double-Targeted Antiproliferative Effect

Emanuele Amata,[†] *Maria Dichiara,*[†] *Emanuela Arena,*[†] *Valeria Pittalà,*[†] *Venerando Pistarà,*[#] *Venera Cardile,*[‡] *Adriana Carol Eleonora Graziano,*[‡] *Aurore Fraix,*[§] *Agostino Marrazzo*[†] *Salvatore Sortino**[§] *and Orazio Prezzavento**[,†]

[†]Department of Drug Sciences, Medicinal Chemistry Section, University of Catania, Viale A. Doria 6, 95125 Catania, Italy.

[§]Department of Drug Sciences, Laboratory of Photochemistry, University of Catania, Viale A. Doria 6, 95125 Catania, Italy.

[#]Department of Drug Sciences, Laboratory of Organic Chemistry, University of Catania, Viale A. Doria 6, 95125 Catania, Italy.

[‡]Department of Biomedical and Biotechnological Sciences, Physiology Section, University of Catania, Via Santa Sofia 97, 95123 Catania, Italy.

ABSTRACT

This contribution reports the synthesis and evaluation of novel hybrid compounds that conjugate a sigma (σ) receptors pharmacophore and a nitric oxide (NO) photodonor. All compounds preserve their capability to generate NO under visible light and possess overall σ receptors nanomolar affinity, with one of them (**8b**) exhibiting remarkable σ_2 receptor selectivity. Compounds **8b**, **11a**, and **11b** were tested on tumorigenic MCF-7 and A2058 cells expressing high levels of σ_2 and σ_1 receptor, respectively. Considerable loss of cell viability was detected under light excitation while negligible effects in the dark were detected. Moreover, they did not show any significant cytotoxicity in the dark or under irradiation on non-tumorigenic NCTC-2544 keratinocytes. NO-induced reduction of cellular viability was demonstrated by in cell NO detection and total nitrite estimation. For the first time, a combination of σ receptors moieties and a NO photodonor is reported, providing distinctive ligands potentially useful for cancer management.

INTRODUCTION

One of the main drawbacks of many conventional anticancer drugs is the induction of significant toxicity to healthy cells.[1,2] To minimize this toxicity issue, a commonly applied strategy is the selective cellular targeting. This is achieved by combining the therapeutic agent with components that specifically bind to biological targets significantly overexpressed in cancer cells.[3] Most of the current research on cellular targeting, is based on the use of antibodies, although, this approach does not lead often to effective intracellular delivery. In contrast, the use of small molecular units as targeting ligands significantly enhances the intracellular drug delivery.[4-6] Another and still poorly investigated form of cellular targeting is based on the

production of cytotoxic species upon light activation.[7] This strategy exploits suitable photochemical precursors that generate cytotoxic agents under the exclusive excitation with biocompatible visible light. This approach does not require, in principle, the selective accumulation of the photoprecursor at the tumor site but only the lack of toxic effects in the dark. Indeed, high selectivity can be achieved by restricting the application of the incident light to the tumor area, and therein confining the release of the cytotoxic species therein. In this context, photodynamic therapy (PDT) is the most used treatment that has found a clinical application, and singlet oxygen ($^1O_2$) is accepted to be the foremost mediator of cytotoxic reactions in cells under PDT treatments.[8,9] Another type of photoactivated therapy is based on the photocontrolled release of nitric oxide (NO) by using suitable NO photodonors (NOPDs).[10-12] Although still confined to the research environment, NO-based therapy holds very promising features helpful in cancer treatment.[13,14] Besides playing multiple roles in the bioregulation of a broad array of physiological processes,[15] NO has also proven to be an effective anticancer agent acting through different mechanisms.[16] However, the role of NO in tumour biology is quite intricate, as this inorganic free radical can act as a tumour progressor or suppressor depending on concentration, duration of exposure, and cells sensitivity to NO.[16] For example, μM range concentrations of NO result in antitumor effects, while pM–nM promote cytoprotective effects.[17]

The development of NOPDs has become of interest due to the superb spatiotemporal control that light-triggering offers if compared to thermal, pH, and metabolic stimuli. Analogously to $^1O_2$, NO presents many advantages over conventional chemotherapeutics, *i.e.* multitarget activity, absence of multidrug resistance problems. Moreover, due to its short lifetime, NO region of action is confined to a short distance from the production site inside the cells (< 200 μm) reducing systemic toxicity effects common to many conventional anticancer drugs.

Differently to $^1O_2$ photogeneration, NO release is independent of O_2 availability. Therefore, NO-based anticancer therapy can successfully complement PDT mainly where this latter may fail, as under the hypoxic conditions typical of some tumours.

Based on the above considerations, the development of molecular conjugates in which a phototherapeutic agent is covalently joined to specific targeting ligands can give intriguing candidates for "double-targeted" cancer therapy. While this approach has already been proposed for PDT agents, only a limited number of examples is known to date regarding targeted NOPDs.[18-24]

Sigma (σ) receptors have been shown to be overexpressed in cancer cells and can be useful for cancer cells targeted drug delivery.[25,26] The σ receptors, firstly introduced as subtypes of the opioid receptors, are now considered a unique class of proteins classified into two subtypes, sigma-1 (σ_1) and sigma-2 (σ_2) with peculiar structure, biological functions, and ligands sensitivity. Indeed, σ_1 binding sites display high affinity for dextro benzomorphan enantiomers like (+)-pentazocine, while levo isomers bind to opioid receptors.[27-29]

The σ_1 receptor has been purified, cloned and crystallized and is well characterized as a chaperone protein at the endoplasmic reticulum (ER)-mitochondria interface where regulates Ca^{2+} signaling and cell survival.[30-33] The σ_1 receptor agonists show neuroprotective, anti-amnestic, and antidepressant effects, while σ_1 receptor antagonists possess modulatory effects on opioid analgesia, as well as antiproliferative, and antiangiogenic activities.[34-40] The σ_1 receptor is highly expressed in lung, breast, and prostate cancer cell lines whereas low levels are found in normal counterpart cells.[41,42]

The σ_2 receptor was purified, revealing its identity as the transmembrane protein 97 (TMEM97), an endoplasmic reticulum-resident transmembrane protein that regulates the sterol

transporter Niemann–Pick disease protein (NPC1).[43] Some quantitative structure-activity relationship (QSAR) models for the determination of the σ_2 receptor binding affinity were setup.[44-47] The σ_2 receptor is found in lungs, liver, and kidney, and it is highly expressed in several malignant tumors including melanoma, neuroblastoma, glioblastoma, breast, and lung cancer.[48-50] Generally, the density of the σ_2 receptor in tumor cell lines is higher than that of the σ_1 receptor, having a ten-fold higher density in proliferating tumor cells than in quiescent tumor cells.[49,51] This evidence indicates that the σ_2 receptor is also an important clinical biomarker for determining the proliferative status of solid tumors. The σ receptors overexpression in tumor cells has led to the development of fluorescent and radiolabeled σ receptor ligands as diagnostic imaging tools using positron emission tomography (PET) or single photon emission computed tomography (SPECT). [^{18}F]ISO-1, a promising PET ligand targeting σ_2 receptor, has been evaluated in clinical trial for the assessment of cellular proliferation in tumors by PET and additional phase I clinical trials on this compound are ongoing.[52-54] Moreover, this overexpression boosted the development of σ receptor ligands derivatized nanocarriers for targeted anticancer drug delivery.[41,49,50,55-59]

On these grounds and motivated by our ongoing interest in developing multifunctional molecular conjugates and nanomaterials photodelivering NO,[10,60,61] in this paper we report the design, synthesis, characterization, and biological evaluation of a new class of molecular hybrids. These latter compounds combine the capability to bind to σ receptors, allowing a preferential accumulation within cancer cells, and the photoregulated release of NO upon visible light excitation.

RESULTS AND DISCUSSION

Design and synthesis. A crucial step when photoresponsive molecular units, such as NOPDs, need to be combined with other functional components, *i.e.* targeting ligands, is the preservation of the photochemical properties of the photoactive center. This is not a trivial result since the response to light of the photoactive unit can be considerably influenced in nature, efficiency or both, by the occurrence of competitive photoprocesses (*i.e.*, photoinduced energy and/or electron transfer, non-radiative deactivation, *etc.*), occurring upon light absorption. With this in mind, we have designed a series of molecular hybrids in which a nitroaniline derivative NOPD developed in our group,[62] and extensively studied[63-67] has been covalently joined to molecules that overall possess the structural determinants for σ receptors recognition.[68,69] In particular, the NOPD 4-nitro-3-trifluoromethyl aniline has been combined with an appropriate σ amino moieties, namely 4-benzylpiperidine or 6,7-dimethoxy-1,2,3,4-tetrahydroisoquinoline, separated by two to five methylene unit spacers (compounds **8**–**11**, Figure 1).

Figure 1. General structure of compounds **8**–**11**

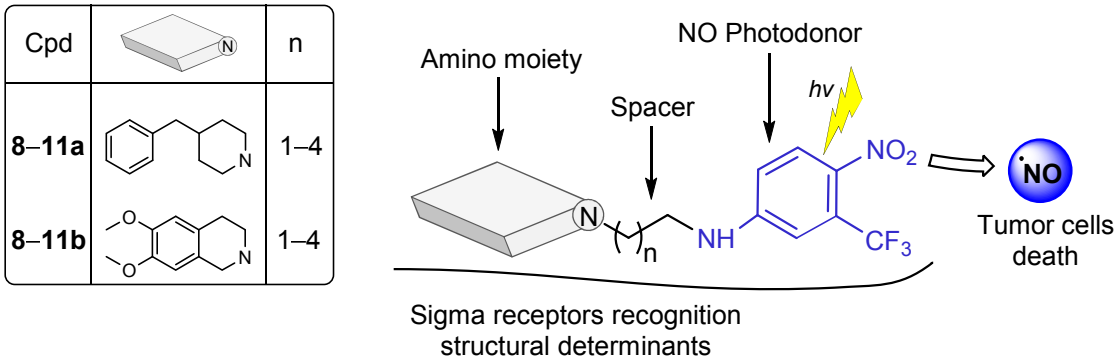

Compounds **8**–**11** were synthesized according to the steps illustrated in Scheme 1. Starting from commercially available 4-fluoro-1-nitro-2-(trifluoromethyl)benzene, intermediates **1** and **2** were obtained with 2-aminoethanol or 5-aminopentan-1-ol and then converted into the

corresponding mesyl derivatives by reaction with mesyl chloride. The mesylated intermediates underwent condensation with 6,7-dimethoxy-1,2,3,4-tetrahydroisoquinoline or 4-benzylpiperidine to give the final compounds **8b** and **11a**–**b**. Compound **9b** was prepared from 4-nitro-3-(trifluoromethyl)aniline via acylation with 3-chloropropionyl-chloride. The resulting chlorine intermediate **3** was coupled with 6,7-dimethoxy-1,2,3,4-tetrahydroisoquinoline to obtain the amide **4b**, which in turn was reduced to the resulting amine **9b** using $LiAlH_4$.

Scheme 1. Synthesis of compounds **8**–**11**.[a]

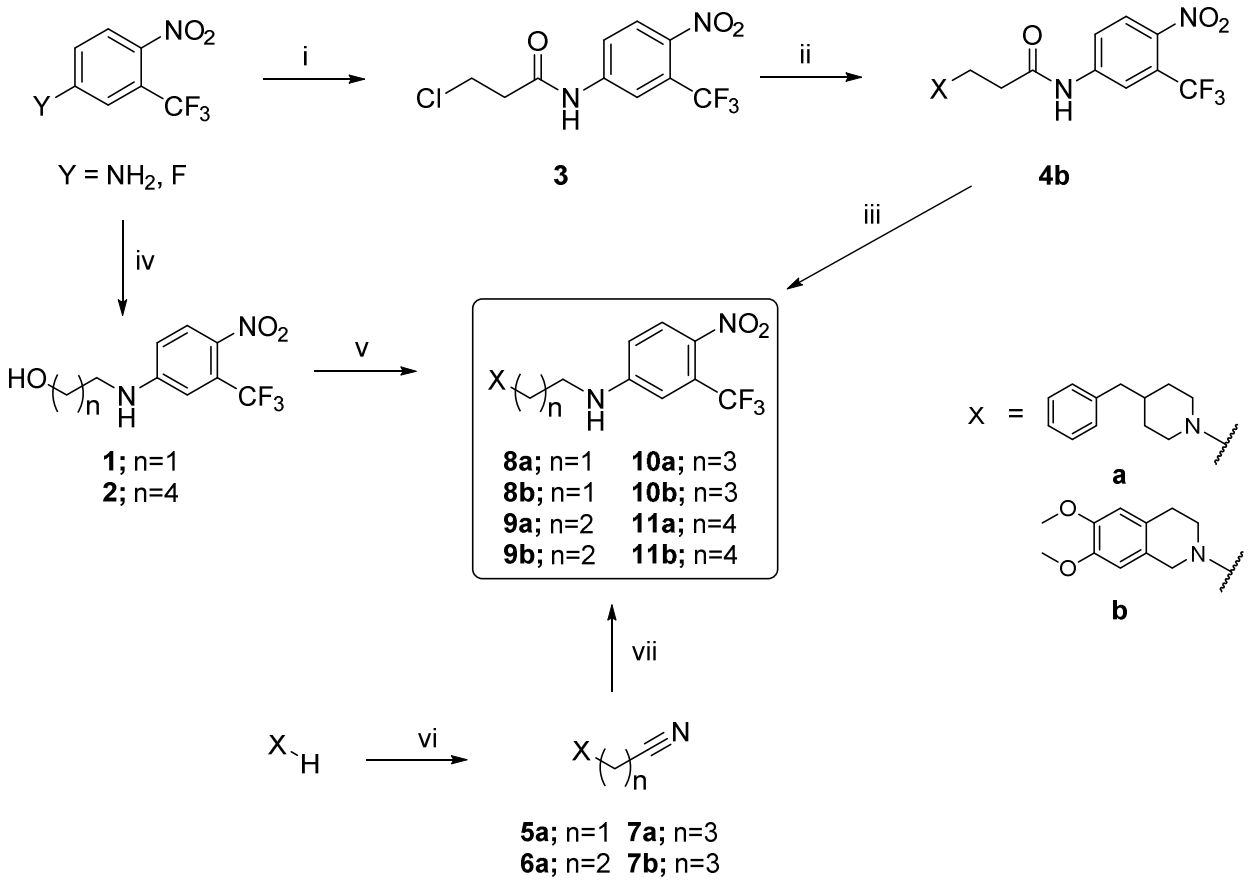

[a]Reagents and conditions: (i) Y=NH_2, $ClCH_2CH_2COCl$, Et_3N, CH_2Cl_2, 0 °C to rt, overnight; (ii) 6,7-dimethoxy-1,2,3,4-tetrahydroisoquinoline, $NaHCO_3$, DMF, 70 °C, overnight; (iii) $LiAlH_4$, THF, N_2, rt, overnight; (iv) Y=F, appropriate amino alcohol, Et_3N, EtOH, 100 °C, 30 min; (v) 1) mesyl chloride, Et_3N, CH_2Cl_2, 0 °C to rt, N_2, 2) appropriate amine, Et_3N, CH_2Cl_2, 0 °C to rt, N_2; (vi) $BrCH_2CN$ or $BrCH_2CH_2CN$ or $BrCH_2CH_2CH_2CN$, NaI, K_2CO_3, DMF, 60 °C, overnight; (vii) 1) $LiAlH_4$, THF, rt, N_2, 2) 4-fluoro-1-nitro-2-(trifluoromethyl)benzene, Et_3N, ACN, 60 °C, overnight.

Conversely, amines **8a**, **9a** and **10a**–**b** were obtained via alkylation of 4-benzylpiperidine or 6,7-dimethoxy-1,2,3,4-tetrahydroisoquinoline with 2-bromoacetonitrile or 3-bromopropanenitrile or 4-bromobutanenitrile to give the corresponding nitrile derivatives **5a**, **6a**, and **7a**–**b**.The latter compounds were reduced with $LiAlH_4$ to give the corresponding diamines and condensed with 4-fluoro-1-nitro-2-(trifluoromethyl)benzene through nucleophilic aromatic substitution to obtain the desired products **8a**, **9a**, and **10a**–**b**.[70-73]

We then investigated how the chemical structure of the amino moieties and their distance from the NO photodonor region influenced the σ receptors affinity and their ability in releasing NO.

Radioligand binding assay. The synthesized compounds bearing a 4-benzylpiperidine (**8a**−**11a**) or a 6,7-dimethoxy-1,2,3,4-tetrahydroisoquinoline moiety (**8b**−**11b**), were evaluated for affinity at both σ_1 and σ_2 receptors through radioligand binding assay (Table 1).

Table 1. σ_1 and σ_2, binding assays of compounds **8**–**11**

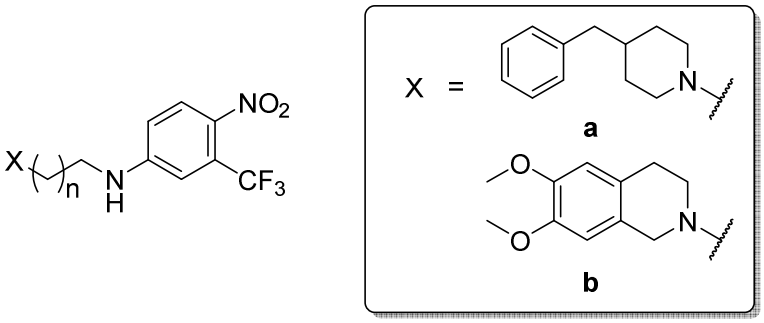

		K_i (nM) ±SD[a]		
Compound	**n**	**σ_1**	**σ_2**	**σ_1/σ_2**
8a	1	40.7 ± 0.95	76.1 ± 1.2	0.53
9a	2	41.6 ± 0.84	22.3 ± 1.0	1.87
10a	3	20.0 ± 1.10	8.4 ± 0.80	2.38
11a	4	40.4 ± 0.81	24 ± 0.85	1.68
8b	1	3,916 ± 205	23.8 ± 1.23	164.5
9b	2	212.4 ± 17	16.2 ± 0.76	13.11

10b	3	37.8 ± 0.91	23.0 ± 0.65	1.64
11b	4	39.4 ± 1.10	25.5 ± 0.78	1.55
Haloperidol	-	2.5 ± 0.40	16.0 ± 1.60	0.16

[a]Each value is the mean ± SD of three determinations.

Within the 4-benzylpiperidine series (**8a**−**11a**), all compounds have shown double digits nanomolar affinity toward both receptor subtypes with $K_i\sigma_1$ in the 20–40 nM range, and $K_i\sigma_2$ in the 8–76 nM range. Compound **10a** demonstrated particular high affinity for both receptor subtypes ($K_i\sigma_1$ = 20.0 nM and $K_i\sigma_2$ = 8.4 nM). The spacer elongation did not alter significantly the binding affinity or selectivity. Compounds bearing the 6,7-dimethoxy-1,2,3,4-tetrahydroisoquinoline (**8b**−**11b**) moiety showed a preference for the σ_2 receptor. Indeed, compound **8b** demonstrated high affinity and selectivity for this receptor subtype with $K_i\sigma_1$ = 3,916 nM and $K_i\sigma_2$ = 23.8 nM, having a σ_1/σ_2 selectivity ratio of 164 fold. The spacer elongation in this series brought to an improvement of the σ_1 receptor affinity while keeping the σ_2 receptor affinity almost unchanged. Indeed, compounds **8b**–**9b** with two or three methylene chain, respectively, showed low affinity for the σ_1 receptor ($K_i\sigma_1$ = 3,916 and 212 nM, respectively), and desirable σ_2 receptor affinity ($K_i\sigma_2$ = 23.8 and 16.2 nM, respectively), while compounds **10b**–**11b** with longer spacer, reported a double digits nanomolar K_i against both receptor subtypes (**10b** $K_i\sigma_1$ = 37.8 nM and $K_i\sigma_2$ = 23 nM; **11b** $K_i\sigma_1$ = 39.4 nM and $K_i\sigma_2$ = 25.5 nM). Affinity at σ_2 receptor has been found in the 16.2–25.5 nM range, thus a clear spacer length effect on σ_2 receptor was not established for this series.

Overall within the designed compounds, the 4-nitro-3-(trifluoromethyl)aniline moiety is well tolerated with regard to σ receptors binding affinity. The series bearing the 4-benzylpiperidine moiety has demonstrated higher affinity against both receptor subtypes. While in the 6,7-dimethoxy-1,2,3,4-tetrahydroisoquinoline series a preference for the σ_2 receptor was observed in those compounds with a shorter spacer. Haloperidol, a typical σ receptors ligand used as

reference compounds, has reported K_i values at both σ receptor subtypes, in accordance with previously published data. With exception of compound **8a** ($K_i\sigma_2$ = 76.1 nM**)**, all derivatives have shown σ_2 receptor affinity (8.4–25.5 nM range) comparable to that of haloperidol ($K_i\sigma_2$ = 16.0 nM).

Spectroscopic and photochemical properties. All compounds synthesized are well soluble in a water:methanol (1:1) mixture. As expected, the nitroaniline chromogenic unit strongly dominates the absorption in the visible region. The molar absorptivity at the λ_{max} for all molecular hybrids is ca. 10.000 M^{-1} cm^{-1}. This value is similar to those already reported for the NO photocage alone ruling out any significant interaction, in the ground state, between the nitroaniline chromogenic unit and the targeting molecular components.

Figure 2 shows the absorption spectra for compounds **8b** and **11a** chosen as representative for the two different targeting motifs having a short and a long spacer, respectively.[62,74]

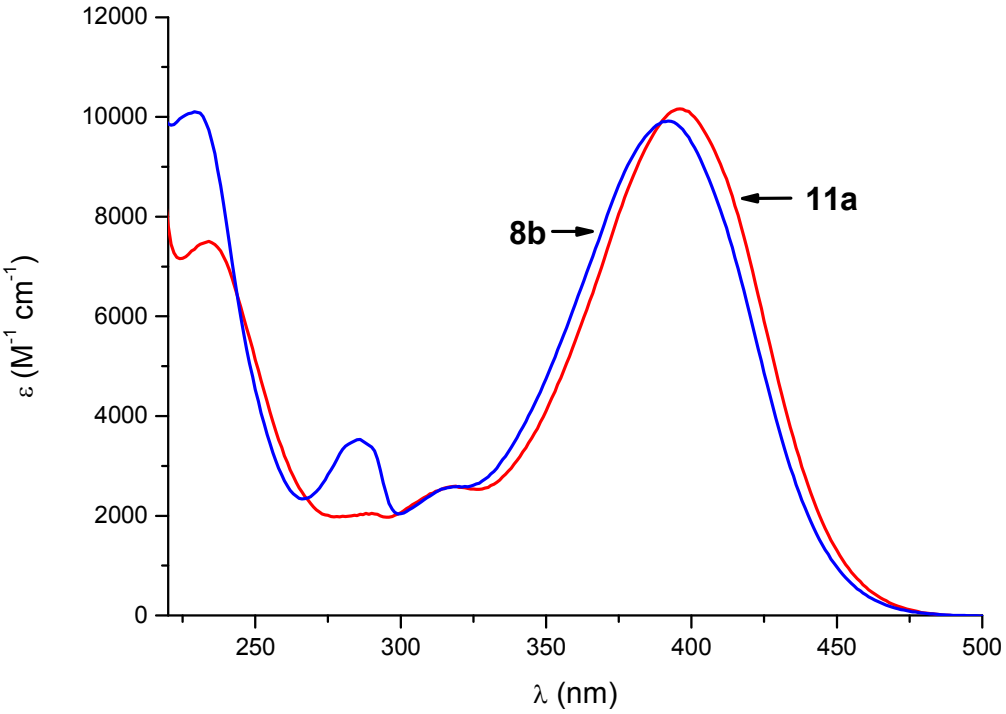

Figure 2. Absorption spectra of **8b** and **11a** in water:methanol (1:1) solution.

As outlined in the design section (*vide supra*), the NOPD photoreleasing capability need to be preserved after its covalent conjugation in order to exploit the NO-induced cytotoxic effects. The most convenient methodology to demonstrate the NO release from the molecular conjugates under visible light irradiation is the direct and real-time monitoring of released NO amount. To this end, we have employed an ultrasensitive NO electrode, which directly detects NO with nM concentration sensitivity by an amperometric technique. In Figure 3 a representative amperogram obtained for compound **11b** is reported. The amperometric measurement gives an unambiguous evidence that the compound is stable in the dark but supplies NO upon illumination with visible light. It should be noted that the release process is strictly regulated by the external light inputs as confirmed by the linear NO generation, which promptly stops as the light turns off and restarts as the illumination turns on again.

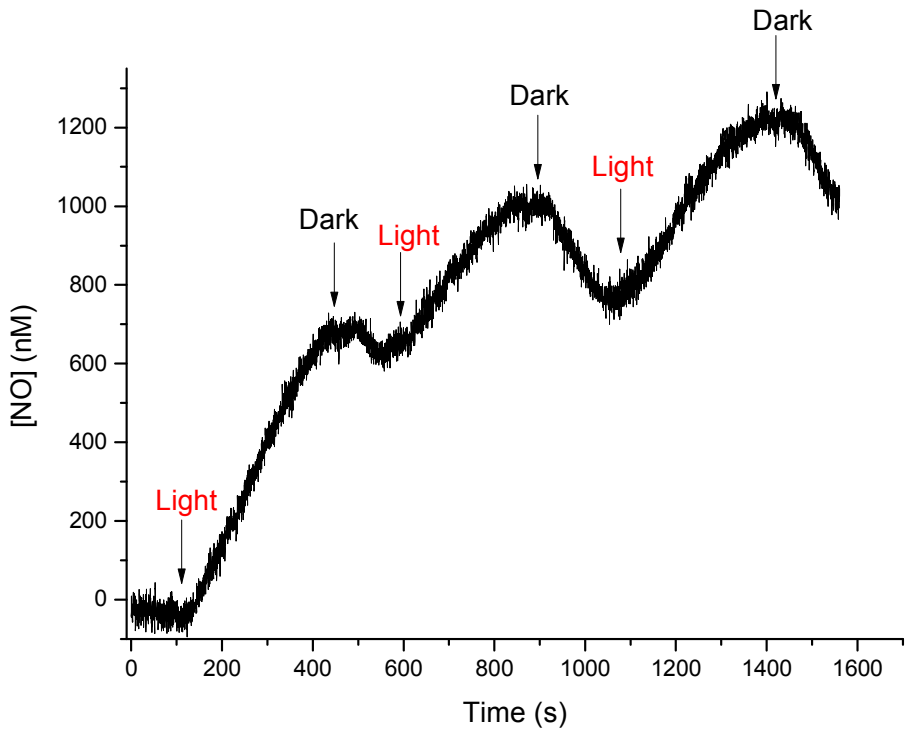

Figure 3. NO release profiles observed upon visible light irradiation (λ_{exc} = 405 nm) of a water:methanol (1:1) solution of **11b** (50 μM).

Of interest is that the absorption spectral changes of **11b** as function of the irradiation time show a photobleaching of the visible band without any significant shift in the absorption maximum (Figure 4). This spectral behavior is in excellent agreement with the photochemical pathway leading to the NO release previously proposed for the single NO photodonor unit and rules out the occurrence of any competitive reaction.

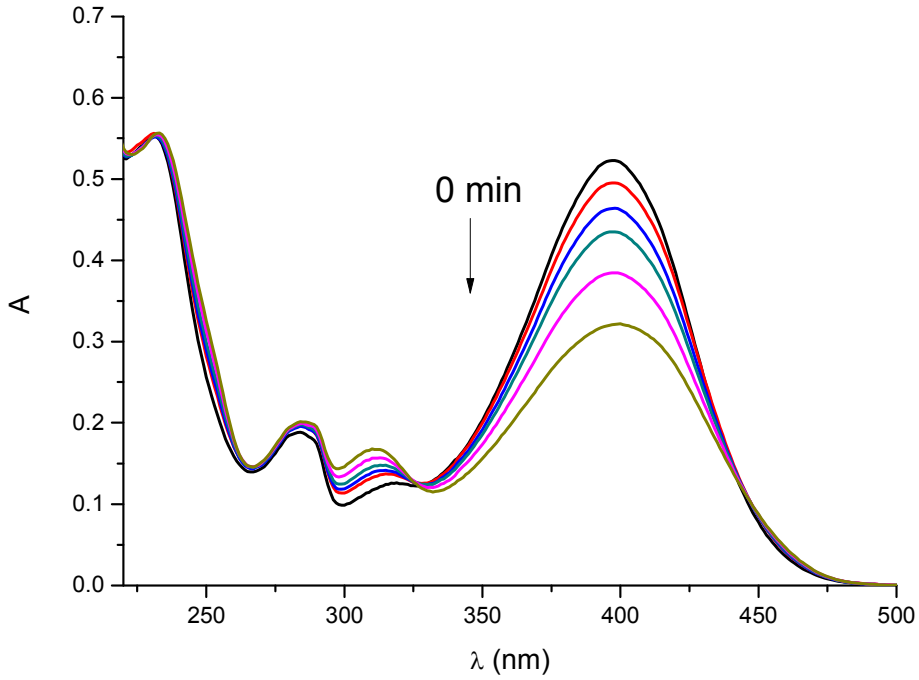

Figure 4. Absorption spectral changes observed upon visible light irradiation (λ_{exc} = 405 nm) of a water:methanol (1:1) solution of **11b** (50 μM) from 0 to 85 min.

All compounds showed a good capability to release NO under photoexcitation, with quantum yields (Φ_{NO}) ranging from ca. 0.01 to 0.03 in the solvent mixture used (Table 2). In particular, while no significant differences were noted in the 4-benzylpiperidine series (**8a**−**11a**), the NO photorelease quantum yields was dependent on the length of the spacer in the 6,7-dimethoxy-1,2,3,4-tetrahydroisoquinoline series (**8b**−**11b**). This behavior can be tentatively attributed to potential quenching effect by photoinduced electron transfer involving the tetrahydroisoquinoline (as an electron donor) and the NO photoreleasing moiety (as an electron acceptor) competitive with the photorelease of NO and taking place more effectively in the compounds with shorter spacers.

Table 2. NO photorelease quantum yields (Φ_{NO}) for compounds **8**−**11**

Compound	Φ_{NO}
8a	0.031
9a	0.025
10a	0.033
11a	0.035
8b	0.010
9b	0.017
10b	0.027
11b	0.034

Cell viability assay

Considering that targeting therapeutic agents should be useful in reducing cytotoxicity in healthy cells, a selected group of molecular hybrids was tested in *in vitro* studies. Tumorigenic and non-tumorigenic cell lines were used to evaluate the compounds putative function as cell death inducers through the photorelease of the cytotoxic concentration of NO. Specifically, given the overexpression of the σ_2 receptor in rapidly proliferating cells compared to quiescent cells, the different concentrations of the representative compounds (**8b**, **11a**, and **11b**) were evaluated in MCF-7 breast adenocarcinoma cell line expressing high levels of σ_2 receptor and very low or even no σ_1 receptor expression.[75] They were also tested in A2058 melanoma cell line, which, in contrast, expresses the σ_1 receptor. Finally, biological tests were also performed on non-tumorigenic skin keratinocytes NCTC-2544 cells.[76] Compound **8b** was selected because of its remarkable affinity and selectivity towards the σ_2 receptor, whereas compounds **11a** and **11b** were selected because of their good affinities for both σ_1 and σ_2 receptors combined with their good NO photoreleasing capabilities.

The first step was the determination of the toxic concentrations of tested compounds against selected cell lines. For this purpose, all cell lines were incubated in the dark, in the presence of

doxorubicin (**12**), **8b**, **11a**, or **11b** for 24 hours (Table 3). The antineoplastic drug **12** was evaluated in order to define cells sensitivity toward death induction. In all cell lines, and in a concentration-dependent manner, compound **12** demonstrated a significant reduction of viability confirming that it does not well discriminate between normal and tumor cells. Compound **12** exhibited EC_{50} values of 15.3, 6.5, and 32.5 μM in MCF-7, A2058, and NCTC-2544 cell lines, respectively.

Table 3. MTT viability test on MCF-7, A2058, and NCTC-2544: EC_{50} in the dark at 24 hours for compounds **12**, **8b**, **11a**, and **11b**.

	EC_{50} (μM)[a] (pEC_{50}±SE)[b]			
Cell line	**12**	**8b**	**11a**	**11b**
MCF-7	15.3 (4.81 ± 0.15)	>100[c] (<4)	14.9 (4.83 ± 0.05)	>100[c] (<4)
A2058	6.5 (5.19 ± 0.34)	>100[c] (<4)	14.2 (4.85 ± 0.05)	>100[c] (<4)
NCTC-2544	32.5 (4.49 ± 0.11)	>100[c] (<4)	15.0 (4.82 ± 0.03)	>100[c] (<4)

[a]EC_{50} values have been calculated with GraphPad Prism 5 for Windows using a nonlinear fit transform sigmoidal dose-response (variable slope). Each value represents the mean of quadruplicate samplings from 96-well microplates ± SEM. Cytotoxicity was measured by the MTT conversion into formazan crystals and expressed as the percentage of viable cell respect to each of untreated controls. Cells were incubated for 24 h in the dark, in the presence of various concentrations of tested compounds; [b]pEC_{50} is defined as the $-\log(EC_{50})$; [c]cell viability reduction lower than 50% at 100 μM.

Compounds **8b** and **11b** have been found considerably safe in all three cell lines evaluated, having shown EC_{50} values >100 μM (inhibition lower than 50% at 100 μM). This trend proves that these compounds are not toxic for both normal and tumor cells at the concentrations evaluated. Conversely, compound **11a** induced a comparable loss of viability in all three cell lines with EC_{50} of 14.9, 14.2, and 15.0 μM in MCF-7, A2058, and NCTC-2544, respectively. According to these results, compound **11a** seems to act as cytotoxic in both normal and tumor cells. This result could be explained by alternative targets involved in the accumulation and/or activity of compound **11a** in the non-tumorigenic NCTC-2544 cell line.

In a second set of experiments, these compounds were evaluated under light irradiation to test their efficacy as NO donors. Different concentrations of tested compounds were applied to cell lines for 24 hours. A potentiation of cytotoxicity was observed when subtoxic concentrations of compound **8b** were combined with light exposure in MCF-7 cell line (Figure 5). At the three tested concentration (10, 25, and 50 μM) compound **8b** exerted a significant reduction of viability under irradiation, in contrast with the negligible mortality observed in the dark (Figure 5, Panel A). Interestingly, when the same experiment was conducted with either A2058 cell line or non-tumorigenic NCTC-2544 cell line, compound **8b** did not induce any significant reduction neither in the dark nor under irradiation (Figure 5, Panels B and C). It is worthy of note that in the selected cell lines the slight reduction of cellular viability observed in the dark was in line with previous observations (Figure 5 and Table 3).

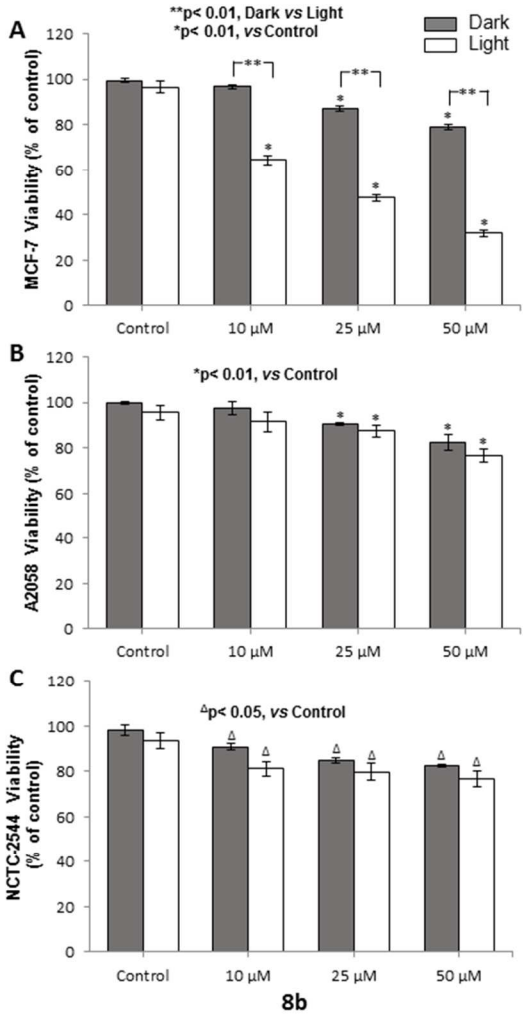

Figure 5. Photodynamic activation of compound **8b**. Various concentrations of compound **8b** were added to MCF-7 (Panel A), A2058 (Panel B), and NCTC-2544 (Panel C) cell lines for 24 hours. Cytotoxicity was determined by MTT assay both in dark condition and after 15 min irradiation. Results are expressed as percentage of cell viability. Each data point represents the mean of quadruplicate samplings from 96-well microplates ± SD.

The decrease of cell viability was associated to light-induced intracellular NO release that was appreciable only in MCF-7 cells treated with compound **8b**. This result was also confirmed by fluorescent method and nitrite quantification (Figure 6, Panel A and B).

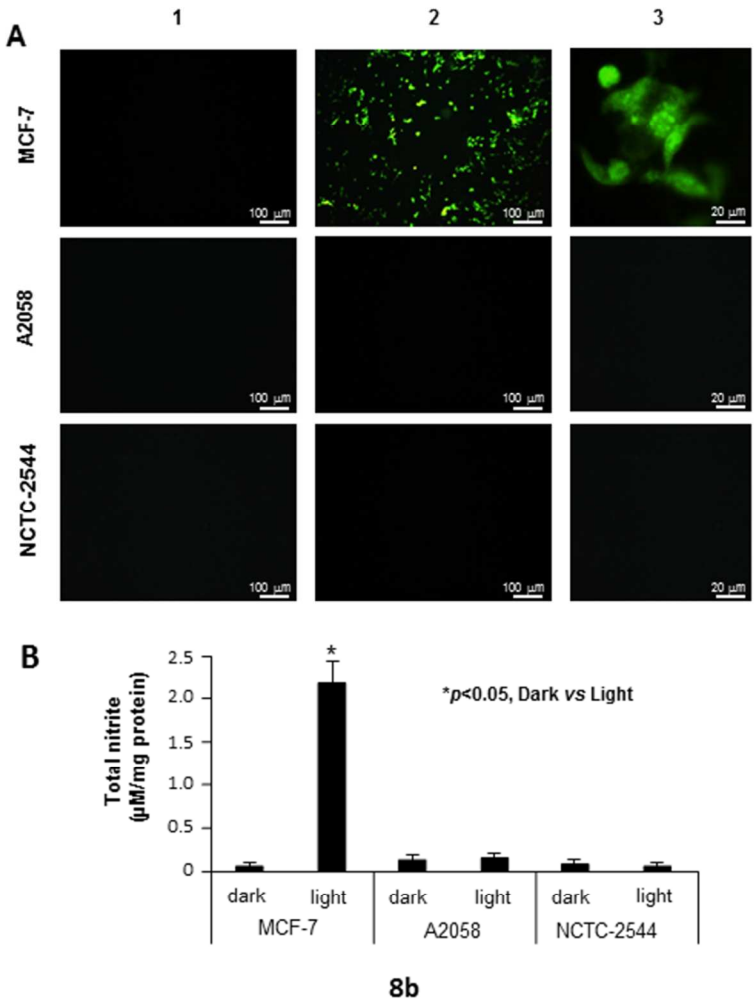

Figure 6. Intracellular NO detection and total nitrite estimation for compound **8b**. (Panel A) Intracellular NO evaluation in cell lines exposed to 50 μM of **8b** determined by DCF-DA and visualized by fluorescence microscopy. Line 1: dark (10x); line 2: light-treated cells (10x); line 3: light-treated cells (40x). (Panel B) Total nitrite content measured using Griess reagent in cells treated with compound **8b** (50 μM) under dark (control) or light conditions.

A similar biological profile was found also for compound **11b**. This conjugate induced a marked and significant loss of viability in MCF-7 cell line (Figure 7, Panel A) at the employed concentrations. Negligible cell mortality was observed both in the dark and under irradiation in A2058 and NCTC-2544 cell lines at the same concentrations (Figure 7, Panels B and C). A

significant light-induced reduction of viability for compound **11b** in A2058 cells was observed only at higher concentrations (data not shown).

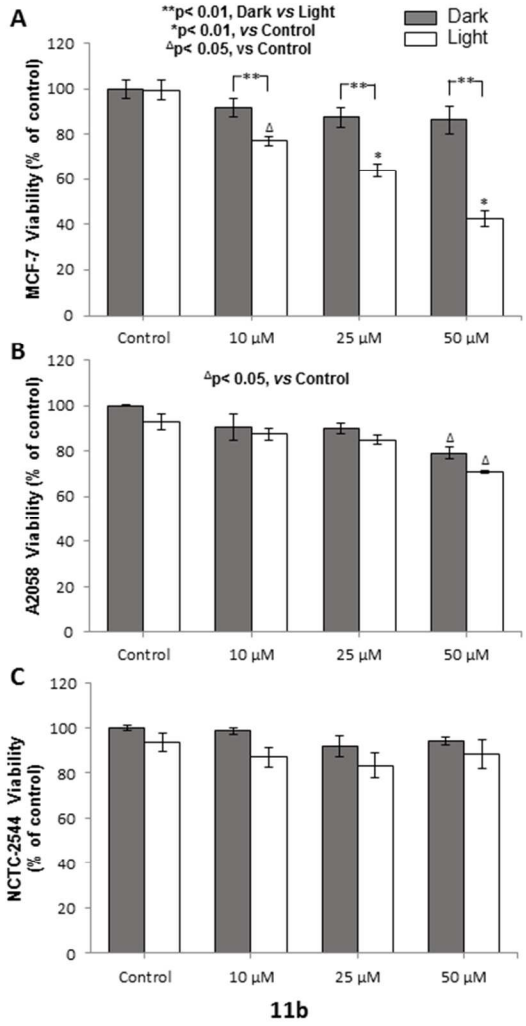

Figure 7. Photodynamic activation of compound **11b**. Various concentrations of compound **11b** were added to MCF-7 (Panel A), A2058 (Panel B), and NCTC-2544 (Panel C) cell lines for 24 hours. Cytotoxicity was determined by MTT assay both in dark condition and after 15 min irradiation. Results are expressed as the percentage of cell viability. Each data point represents the mean of quadruplicate samplings from 96-well microplates ± SD.

An enhanced intracellular NO generation (Figure 8, Panel A) and accumulation of nitrite content (Figure 8, Panel B) were found in light-exposed and **11b**-treated MCF-7 cells.

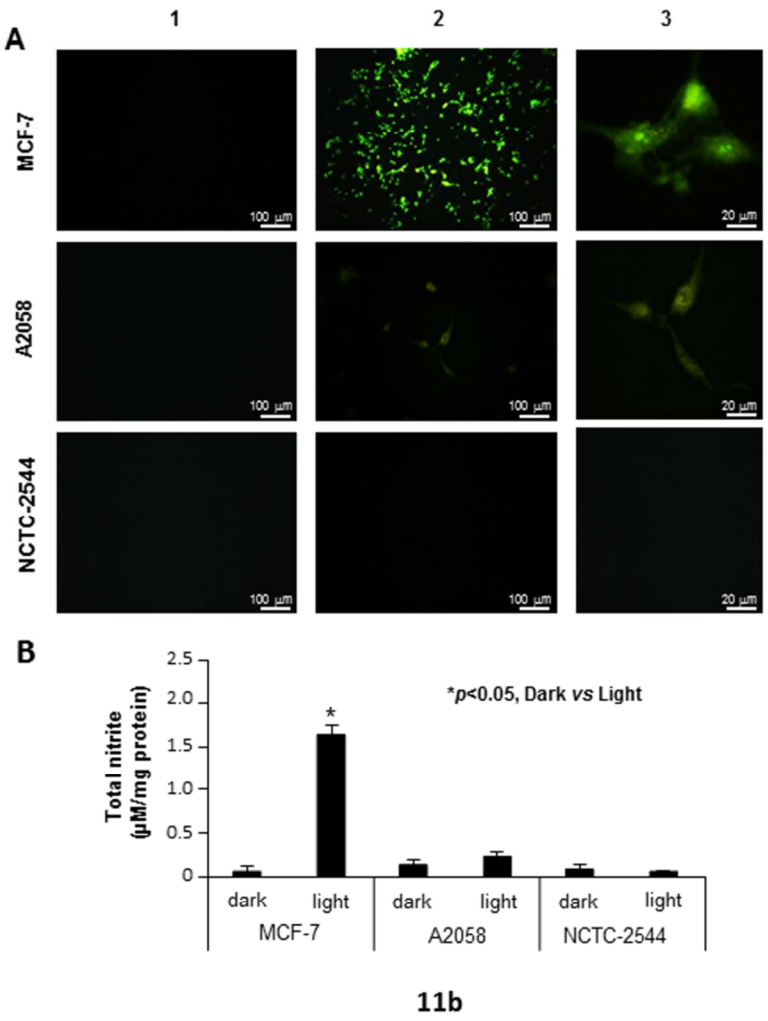

Figure 8. Intracellular NO detection and total nitrite estimation for compound **11b**. (Panel A) Intracellular NO evaluation in cell lines exposed to 50 µM of **11b** determined by DCF-DA and visualized by fluorescence microscopy. Line 1: dark (10x); line 2: light-treated cells (10x); line 3: light-treated cells (40x). (Panel B) Total nitrite content measured using Griess reagent in cells treated with compound **11b** (50 µM) under dark (control) or light conditions.

Regarding compound **11a**, we have to take into account its considerable reduction of the viability in the selected cell lines in the dark (Table 3). Thus, this conjugate was evaluated at lower concentrations with respect to **8b** and **11b** (Figure 9). In MCF-7 cell line, compound **11a** produced a significant photoinduced loss of cellular viability at the four non-toxic concentrations

employed, in contrast to the negligible effect observed in the dark (Figure 9, Panel A). The experiment performed in the A2058 cell line showed an appreciable light-induced mortality at 1.0 and 10 μM (Figure 9, Panel B). No relevant dark or photoinduced mortality was observed when **11a** was incubated with the non-tumorigenic NCTC-2544 cell line at the selected concentrations (Figure 9, Panel C).

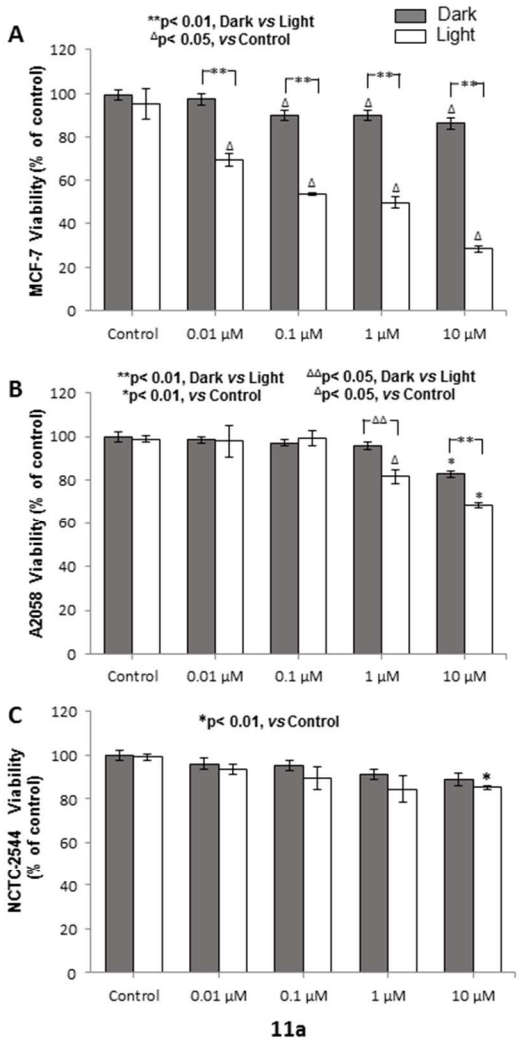

Figure 9. Photodynamic activation of compound **11a**. Various concentrations of compound **11a** were added to MCF-7 (Panel A), A2058 (Panel B), and NCTC-2544 (Panel C) cell lines for 24 hours. Cytotoxicity was determined by MTT assay both in dark condition and after 15 min

irradiation. Results are expressed as the percentage of cell viability. Each data point represents the mean of quadruplicate samplings from 96-well microplates ± SD.

The NO production and the nitrite accumulation were enhanced in MCF-7 and A2058 cells after incubation with 10 μM of **11a** and light irradiation (Figure 10, Panel A and B).

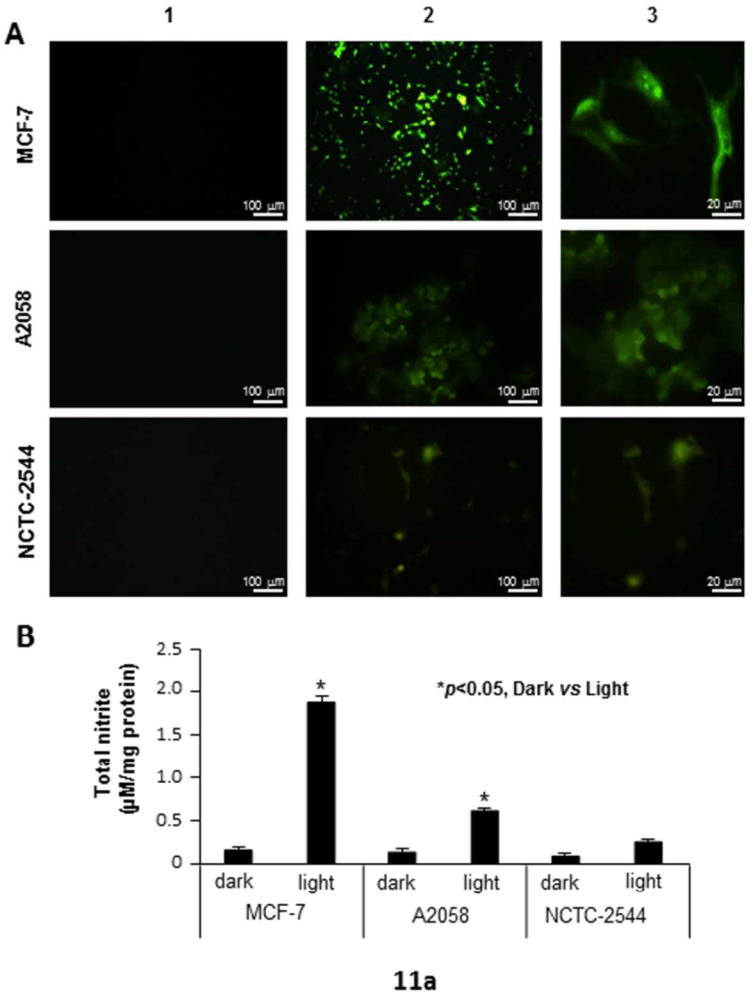

Figure 10. Intracellular NO detection and total nitrite estimation for compound **11a**. (Panel A) Intracellular NO evaluation in cell lines exposed to 10 μM of **11a** determined by DCF-DA and visualized by fluorescence microscopy. Line 1: dark (10x); line 2: light-treated cells (10x); line 3: light-treated cells (40x). (Panel B) Total nitrite content measured using Griess reagent in cells treated with compound **11a** (10 μM) under dark (control) or light conditions.

CONCLUSION

The here reported compounds combine a high σ receptors binding affinity with the capability to release NO upon visible light excitation. Compounds **8b** and **11b** induced a marked loss of viability in tumorigenic MCF-7 cell line under light irradiation, whereas compound **11a** exhibited the same effect on both MCF-7 and A2058 cell lines. The same group of compounds showed negligible cell mortality of non-tumorigenic NCTC-2544 cells at chosen concentrations, both in the dark and under irradiation. The NO-induced reduction of cellular viability was also quantitatively and qualitatively demonstrated by in cell intracellular NO detection and total nitrite estimation. To the best of our knowledge, this is the first time that a successful combination of σ receptors moieties and a NO photodonor is reported, providing distinctive ligands with potential beneficial effect in the treatment of neoplastic disorders

EXPERIMENTAL SECTION

General remarks. Reagent grade chemicals were purchased from Sigma-Aldrich (St. Louis, MO, USA) or Merck (Darmstadt, Germany) and were used without further purification. All reactions involving air-sensitive reagents were performed under nitrogen in oven-dried glassware using the syringe-septum cap technique. Flash chromatography purification was performed on a Merck silica gel 60 0.040–0.063 mm (230–400 mesh) stationary phase. Nuclear magnetic resonance spectra (^{1}H NMR recorded at 200 and 500 MHz) were obtained on VARIAN INOVA spectrometers using $CDCl_3$, DMSO-*d*6 or CD_3OD. TMS was used as an internal standard. Chemical shifts (δ) are given in parts per million (ppm), and coupling constants (*J*) in Hertz

(Hz). The following abbreviations are used to designate the multiplicities: s = singlet, d = doublet, t = triplet, q = quartet, quint = quintet, m = multiplet, br = broad. The purity of all tested compounds, whether synthesized or purchased, reached at least 95% as determined by microanalysis (C, H, N) that was performed on a Carlo Erba instrument model E1110; all the results agreed within ± 0.4% of the theoretical values. Reactions were monitored by thin-layer chromatography (TLC) performed on 0.25 mm silica gel Merck 60 F_{254} coated aluminum plates; the spots were visualized by UV light. UV-Vis spectra absorption spectra were recorded with a JascoV-560 spectrophotometer. LCMS analysis was performed using a Perkin Elmer Flexar FX-10 UHPLC System (software Analyst 1.6.1, columns Waters X-Terra RP18 3.0x150mm, 3.5µm or Thermo Fisher Scientific Hypersil WP-300 C8 4.6x100mm, 5.0µm), with single-wavelength UV–visible detector and API 2000 LC/MS/MS System AB Sciex (electrospray ionization). Compounds nomenclature were generated with ChemBioDraw Ultra version 16.0.0.82.

General procedure for the nitrile formation (Procedure A). In a DMF (24 mL) solution of the appropriate amine (8.71 mmol), K_2CO_3 (13.06 mmol), NaI (0.043 mmol), and the appropriate bromo nitrile (8.71 mmol) were added and the reaction mixture was refluxed for 3 h at 60 °C. After the reaction was complete, the solvent was evaporated to dryness, the residue was dissolved in CH_2Cl_2 (30 mL), washed with a saturated solution of $NaHCO_3$ (2 x 20 mL), and brine (1 x 20 mL). The organic phase was dried with anhydrous Na_2SO_4, concentrated, and the crude product was purified via silica gel chromatography to give the desired product. Products synthesized according to Procedure A: **5a**, **6a**, and **7a**–**b**.

General procedure for the amine preparation (Procedure B). To a solution of the appropriate nitrile (1.4 mmol) in dry THF (6 mL), $LiAlH_4$ (1M in THF, 4.20 mmol) was added dropwise at 0

°C under N_2 atmosphere and the resulting mixture was allowed to warm to room temperature. After 2 h stirring, the reaction was quenched with 1M NaOH (3 mL) at 0 °C, filtered through Celite, and washed with MeOH. The solution was concentrated under reduced pressure and dissolved in CH_2Cl_2. The organic phase was dried over anhydrous Na_2SO_4 and concentrated to give the crude amino product that was used as it without any further purification. To the crude product, dissolved in ACN (3 mL), 4-nitro-3-(trifluoromethyl)aniline (1.40 mmol) in ACN (3 mL) and Et_3N (1.54 mmol) were added. The resulting mixture was placed in an oil bath at 60 °C and left to react overnight. After the reaction was complete, the mixture was washed with hexane. The ACN solution was then evaporated to dryness and the residue purified via flash chromatography. Products synthesized according to Procedure B: **8a**, **9a**, and **10a**–**b**.

General procedure for amine preparation (Procedure C). A solution of the appropriate amino alcohol (1.07 mmol) and Et_3N (2.14 mmol) in CH_2Cl_2 (5 mL) was cooled to 0 °C under N_2 atmosphere. Methanesulfonyl chloride (1.07 mmol) dissolved in CH_2Cl_2 (4 mL) was added and the reaction mixture was allowed to warm to room temperature for 30 min while stirring. The mixture was cooled to 0 °C and a solution of the appropriate amine (2.14 mmol) and Et_3N (4.28 mmol) in CH_2Cl_2 (2 mL) was added. After 70 h, the mixture was washed with a saturated solution of $NaHCO_3$ (1 x 10 mL) and brine (1 x 10 mL). The organic phase was dried over anhydrous Na_2SO_4 and concentrated. The crude product was dissolved in EtOAc, washed with a 0.2 N water solution of H_2SO_4 and the mixture was filtered. The residue was washed with EtOAc/CH_2Cl_2 and left to dry. Then, it was dissolved in EtOAc and washed with $NaHCO_3$ (1 x 10 mL) and brine (1 x 10 mL). The organic phase was dried over anhydrous Na_2SO_4, concentrated and the crude product purified via flash chromatography to give the desired product. Products synthesized according to Procedure C: **8b**, and **11a**–**b**.

2-((4-Nitro-3-(trifluoromethyl)phenyl)amino)ethanol (**1**). To a solution of 4-nitro-3-(trifluoromethyl)aniline (1.43 mmol, 0.30 g) in EtOH (5 mL), the appropriate 2-aminoethanol (7.17 mmol, 0.43 mL) and Et_3N (1.43 mmol, 0.20 mL) were added. After the reaction was complete, the mixture was concentrated and the residue was triturated with water and filtered under vacuum to give the compound **1** as yellow solid (yield: 72%). ^{1}H NMR (500 MHz, CD_3OD) δ 7.92 (d, *J* = 9.2 Hz, 1H), 6.94 (d, *J* = 2.4 Hz, 1H), 6.71 (dd, *J* = 2.4, 9.2 Hz, 1H), 3.64 (t, *J* = 5.8 Hz, 2H), 3.25 (t, *J* = 5.8 Hz, 2H). LCMS found 250.3, $[M + H]^+$.

5-((4-Nitro-3-(trifluoromethyl)phenyl)amino)pentan-1-ol (**2**). To a solution of 4-nitro-3-(trifluoromethyl)aniline (1.43 mmol, 0.30 g) in EtOH (5 mL), the appropriate 5-aminopentan-1-ol (4.29 mmol, 0.44 g) and Et_3N (1.43 mmol, 0.20 mL) were added. After the reaction was complete, the mixture was concentrated and the residue was dissolved in EtOAc, washed with a saturated solution of $NaHCO_3$ (1 x 10 mL) and brine (1 x 10 mL). The combined organic extracts were dried over anhydrous Na_2SO_4 and concentrated affording compound **2** as a yellow oil (yield: 98%). ^{1}H NMR (200 MHz, $CDCl_3$) δ 8.02 (d, *J* = 9.2 Hz, 1H), 6.87 (d, *J* = 2.6 Hz, 1H), 6.64 (dd, *J* = 2.6, 9.2 Hz, 1H), 4.81 (br. s., 1H), 3.70 (t, *J* = 6.0 Hz, 2H), 3.24 (q, *J* = 6.70 Hz, 2H), 1.42 – 1.82 (m, 6H). LCMS found 292.6, $[M + H]^+$.

3-Chloro-N-(4-nitro-3-(trifluoromethyl)phenyl)propanamide (**3**). To a solution of 4-nitro-3-(trifluoromethyl)aniline (4.85 mmol, 1 g) in dry CH_2Cl_2 (15 mL), 3-chloropropionyl-chloride (5.82 mmol, 0.55 mL) and Et_3N (5.82 mmol, 0.81 mL) were added dropwise at 0 °C under N_2 atmosphere. The reaction mixture was stirred at room temperature overnight. After the reaction was complete, it was cooled to 0 °C and quenched with water and a saturated solution of $NaHCO_3$ (3 mL) dropwise. The CH_2Cl_2 solution was washed with a saturated solution of $NaHCO_3$ (2 x 10 mL), brine (1 x 10 mL) and dried over anhydrous Na_2SO_4. The solvent was

concentrated under vacuum and the crude product was purified via silica gel chromatography, eluting with 25% EtOAc in Hexane to give the desired product as white solid (yield: 60%). ^{1}H NMR (200 MHz, 47 DMSO-*d*6) δ 8.01 – 8.17 (m, 2H), 7.82 – 7.96 (m, 1H), 3.75 (t, *J* = 6.3 Hz, 2H), 2.77 (t, *J* = 6.3 Hz, 2H). MS found 296.5, $[M + H]^+$.

3-(6,7-Dimethoxy-3,4-dihydroisoquinolin-2(1H)-yl)-N-(4-nitro-3-(trifluoromethyl)phenyl)propanamide (**4b**). To a solution of compound **3** (2.15 mmol, 0.64 g) in DMF (16 mL) were added 6,7-dimethoxy-1,2,3,4-tetrahydroisoquinoline (2.15 mmol, 0.5 g) and $NaHCO_3$ (5.37 mmol, 0.45 g). The mixture was heated to 70 °C and stirred overnight. After the reaction was complete, DMF was evaporated under vacuum and the residue was dissolved in CH_2Cl_2 (40 mL), washed with a saturated solution of $NaHCO_3$ (2 x 15 mL) and brine (1x15 mL). The solvent was dried over anhydrous Na_2SO_4, concentrated under vacuum and the crude was purified by flash chromatography, eluting with 5 to 10% Hexane in EtOAc and finally with 100% EtOAc to give the desired product as yellow solid (yield: 47%). ^{1}H NMR (200 MHz, $CDCl_3$) δ 7.65 – 7.93 (m, 3H), 6.69 (s, 1H), 6.57 (s, 1H), 3.81 – 3.96 (m, 6H), 3.76 (s, 2H), 2.90 – 3.03 (m, 6H), 2.58 – 2.73 (m, 2H). LCMS found 453.0, $[M + H]^+$.

2-(4-Benzylpiperidin-1-yl)acetonitrile (**5a**). The compound has been prepared following procedure A and using 2-bromoacetonitrile (11.41 mmol, 0.76 mL). The crude product was purified via silica gel chromatography, eluting with 10 to 40% EtOAc in Hexane to give compound **5a** as a white solid (yield: 75%). ^{1}H NMR (500 MHz, $CDCl_3$) δ 7.25 – 7.30 (m, 2H), 7.17 – 7.22 (m, 1H), 7.11 – 7.15 (m, 2H), 3.50 (s, 2H), 2.73 – 2.80 (m, 2H), 2.54 (d, *J* = 7.34 Hz, 2H), 2.28 (dt, *J* = 2.7, 11.6 Hz, 2H), 1.67 – 1.73 (m, 2H), 1.50 – 1.61 (m, 1H), 1.25 – 1.36 (m, 2H). LCMS found 214.2, $[M + H]^+$.

3-(4-Benzylpiperidin-1-yl)propanenitrile (**6a**). The compound has been prepared following procedure A and using 3-bromopropanenitrile (11.41 mmol, 0.95 mL). The mixture was stirred at 60 °C overnight. The crude product was purified via silica gel chromatography, eluting with 10 to 50% EtOAc in Hexane to give compound **6a** as a clear oil (yield: 49%). ^{1}H NMR (500 MHz, $CDCl_3$) δ 7.25 – 7.30 (m, 2H), 7.16 – 7.21 (m, 1H), 7.10 – 7.15 (m, 2H), 2.86 (br. d, *J* = 11.2 Hz, 2H), 2.67 (t, *J* = 7.3 Hz, 2H), 2.53 (d, *J* = 7.1 Hz, 2H), 2.48 (t, *J* = 7.1 Hz, 2H), 1.99 (dt, *J* = 2.5, 11.6 Hz, 2H), 1.64 (br. d, *J* = 13.2 Hz, 2H), 1.46 – 1.57 (m, 1H), 1.23 – 1.35 (m, 2H). LCMS found 228.5, $[M + H]^+$.

4-(4-Benzylpiperidin-1-yl)butanenitrile (**7a**). The compound has been prepared following procedure A and using 4-bromobutanenitrile (11.41 mmol, 1.13 mL). The mixture was stirred at 60 °C overnight. The crude product was purified via silica gel chromatography, eluting with 100% EtOAc to give compound **7a** as a yellow oil (yield: 18%). ^{1}H NMR (500 MHz, $CDCl_3$) δ 7.25 – 7.30 (m, 2H), 7.16 – 7.21 (m, 1H), 7.11 – 7.15 (m, 2H), 2.83 (br. d, *J* = 11.5 Hz, 2H), 2.53 (d, *J* = 7.1 Hz, 2H), 2.35 – 2.42 (m, 4H), 1.88 (dt, *J* = 2.2, 11.7 Hz, 2H), 1.80 (quint, *J* = 7.0 Hz, 2H), 1.62 (br. d, *J* = 13.7 Hz, 2H), 1.46 – 1.56 (m, 1H), 1.22 – 1.32 (m, 2H). LCMS found 242.0, $[M + H]^+$.

4-(6,7-Dimethoxy-3,4-dihydroisoquinolin-2(1H)-yl)butanenitrile (**7b**). The compound has been prepared following procedure A and using 4-bromobutanenitrile (8.71 mmol, 0.86 mL). The crude product was purified via silica gel chromatography, eluting with 30% EtOAc in Hexane, to give compound **7b** as a white solid (yield: 78 %). ^{1}H NMR (200 MHz, $CDCl_3$) δ 6.60 (s, 1H), 6.52 (s, 1H), 3.79 – 3.90 (m, 6H), 3.55 (br. s, 2H), 2.77 – 2.87 (m, 2H), 2.68 – 2.76 (m, 2H), 2.63 (t, *J* = 6.7 Hz, 2H), 2.48 (t, *J* = 7.0 Hz, 2H), 1.94 (quint, *J* = 7.0 Hz, 2H). LCMS found 260.4, $[M + H]^+$.

N-(2-(4-Benzylpiperidin-1-yl)ethyl)-4-nitro-3-(trifluoromethyl)aniline (**8a**). The compound has been prepared following procedure B and using 2-(4-benzylpiperidin-1-yl)acetonitrile (**5a**) (1.37 mmol, 0.29 g). The crude product was purified by flash chromatography in EtOAc to give the final compound as yellow oil (yield: 54%). ^{1}H NMR (200 MHz, $CDCl_3$) δ 8.02 (d, *J* = 9.0 Hz, 1H), 7.05 – 7.37 (m, 5H), 6.89 (d, *J* = 2.4 Hz, 1H), 6.63 (dd, *J* = 2.4, 9.0 Hz, 1H), 5.52 (br. s., 1H), 3.22 (q, *J* = 5.0 Hz, 2H), 2.86 (d, *J* = 10.5 Hz, 2H), 2.46 – 2.67 (m, 4H), 1.96 (t, *J* = 11.4 Hz, 2H), 1.46 – 1.75 (m, 3H), 1.14 – 1.41 (m, 2H). Anal. calcd for: $C_{21}H_{24}F_3N_3O_2$: C, 61.91; H, 5.94; N, 10.31. Found: C, 61.78; H, 5.96; N, 10.40. LCMS found 407.4, $[M + H]^+$.

*N-(2-(6,7-Dimethoxy-3,4-dihydroisoquinolin-2(1H)-yl)ethyl)-4-nitro-3-(trifluoromethyl)anilin*e (**8b**). The compound has been prepared following procedure C and using 2-((4-nitro-3-(trifluoromethyl)phenyl)amino)ethanol (**1**) (1.07 mmol, 0.26 g) and 6,7-dimethoxy-1,2,3,4-tetrahydroisoquinoline (2.14 mmol, 0.41 g). The crude product was purified by flash chromatography eluting 5% MeOH in EtOAc to give compound **8b** as a yellow solid (yield: 35%). ^{1}H NMR (200 MHz, $CDCl_3$) δ 8.01 (d, *J* = 9.2 Hz, 1H), 6.89 (d, *J* = 2.2 Hz, 1H), 6.60 – 6.69 (m, 2H), 6.54 (s, 1H), 5.58 (br. s., 1H), 3.78 – 3.93 (m, 6H), 3.62 (s, 2H), 3.28 – 3.42 (m, 2H), 2.73 – 2.93 (m, 6H). Anal. calcd for: $C_{20}H_{22}F_3N_3O_4$: C, 56.47; H, 5.21; N, 9.88. Found: C, 56.29; H, 5.22; N, 9.78. LCMS found 425.0, $[M + H]^+$.

N-(3-(4-Benzylpiperidin-1-yl)propyl)-4-nitro-3-(trifluoromethyl)aniline (**9a**). The compound has been prepared following procedure B and using 3-(4-benzylpiperidin-1-yl)propanenitrile (**6a**) (1.37 mmol, 0.31 g). The crude product was purified by flash chromatography, eluting with 5 to 10% MeOH in EtOAc to give the final compound as yellow oil (yield: 20%). H^1 NMR (200 MHz, $CDCl_3$) δ 8.02 (d, *J* = 9.2 Hz, 1H), 7.06 – 7.42 (m, 5H), 6.80 (d, *J* = 2.4 Hz, 1H), 6.51 (dd, *J* = 2.4, 9.2 Hz, 1H), 3.21 – 3.35 (m, 2H), 2.98 (br. d, *J* = 11.4 Hz, 2H), 2.45 – 2.63 (m, 4H), 1.49

– 2.07 (m, 7H), 1.15 – 1.40 (m, 2H). Anal. calcd for: $C_{22}H_{26}F_3N_3O_2$: C, 62.70; H, 6.22; N, 9.97. Found: C, 62.90; H, 6.21; N, 10.03. LCMS found 421.1, $[M + H]^+$.

N-(3-(6,7-Dimethoxy-3,4-dihydroisoquinolin-2(1H)-yl)propyl)-4-nitro-3-(trifluoromethyl)aniline (**9b**). To a solution of compound **4b** (0.57 mmol, 0.28 g) in dry THF (8.7 mL), $LiAlH_4$ (1M in THF, 1.2 mL) was added dropwise under N_2 atmosphere. The reaction mixture was allowed to warm to room temperature and stirred overnight. After the reaction was complete, it was cooled to 0°C and quenched with water (2 mL) dropwise, followed by filtration through Celite washing with MeOH. The solution was concentrated under reduced pressure and dissolved in CH_2Cl_2. The organic phase was dried over anhydrous Na_2SO_4, concentrated under vacuum and the residue was purified by flash chromatography eluting with EtOAc to give the desired product as yellow solid (yield: 27%). ^{1}H NMR (500 MHz, $CDCl_3$) δ 7.97 (d, J = 9.1 Hz, 1H), 6.72 (d, J = 2.5 Hz, 1H), 6.65 (s, 1H), 6.53 (s, 1H), 6.51 (dd, J = 2.5, 9.1 Hz, 1H), 3.88 (s, 3H), 3.85 (s, 3H), 3.68 (s, 2H), 3.36 (t, J = 6.1 Hz, 2H), 2.89 – 2.93 (m, 2H), 2.83 – 2.88 (m, 2H), 2.81 (t, J = 6.0 Hz, 2H), 1.98 (quint, J = 6.0 Hz, 2H). Anal. calcd for: $C_{21}H_{24}F_3N_3O_4$: C, 57.40; H, 5.51; N, 9.56. Found: C, 57.58; H, 5.53; N, 9.66. LCMS found 439.5, $[M + H]^+$.

N-(4-(4-Benzylpiperidin-1-yl)butyl)-4-nitro-3-(trifluoromethyl)aniline (**10a**). The compound has been prepared following procedure B and using 4-(4-benzylpiperidin-1-yl)butanenitrile (**7a**) (1.37 mmol, 0.332 g). For the work-up EtOAc was used instead of CH_2Cl_2 due solubility reasons. The crude product was purified via flash chromatography, eluting with 100% EtOAc to give the final compound as yellow oil (yield: 35%). ^{1}H NMR (200 MHz, $CDCl_3$) δ 8.04 (d, J = 9.2 Hz, 1H), 7.08 – 7.35 (m, 5H), 6.86 (d, J = 2.5 Hz, 1H), 6.57 (dd, J = 2.5, 9.2 Hz, 1H), 3.10 – 3.24 (m, 2H), 2.91 (br. d, J = 11.7 Hz, 2H), 2.56 (d, J = 7.0 Hz, 2H), 2.35 (t, J = 6.3 Hz, 2H), 1.45 – 1.98

(m, 9H), 1.24 – 1.43 (m, 2H). Anal. calcd for: $C_{23}H_{28}F_3N_3O_2$: C, 63.43; H, 6.48; N, 9.65. Found: C, 63.52; H, 6.50; N, 9.47. LCMS found 435.6, $[M + H]^+$.

N-(4-(6,7-Dimethoxy-3,4-dihydroisoquinolin-2(1H)-yl)butyl)-4-nitro-3-(trifluoromethyl)aniline (**10b**). The compound has been prepared following procedure B and using 4-(6,7-dimethoxy-3,4-dihydroisoquinolin-2(1H)-yl)butanenitrile (**7b**) (1.40 mmol, 0.36 g). The crude product was purified via flash chromatography in EtOAc to give the final compound as yellow solid (yield: 46%). ^{1}H NMR (200 MHz, $CDCl_3$) δ 7.91 (d, J = 9.2 Hz, 1H), 6.51 – 6.69 (m, 3H), 6.31 – 6.44 (m, 1H), 3.81 – 3.90 (m, 6H), 3.59 (s, 2H), 3.12 – 3.25 (m, 2H), 2.70 – 2.95 (m, 4H), 2.58 (t, J = 5.4 Hz, 2H), 1.71 – 1.92 (m, 4H). Anal. calcd for: $C_{22}H_{26}F_3N_3O_4$: C, 58.27; H, 5.78; N, 9.27. Found: C, 58.36; H, 5.79; N, 9.13. LCMS found 453.7, $[M + H]^+$.

N-(5-(4-Benzylpiperidin-1-yl)pentyl)-4-nitro-3-(trifluoromethyl)aniline (**11a**). The compound has been prepared following procedure C and using 5-(4-nitro-3-(trifluoromethyl)phenyl)amino)pentan-1-ol (**2**) (1.07 mmol, 0.31 g) and 4-benzylpiperidine (2.14 mmol, 0.37 g). The crude product was purified by flash chromatography, eluting with 3 to 4% MeOH in EtOAc to give compound **11a** as a yellow oil (yield: 36%). ^{1}H NMR (200 MHz, $CDCl_3$) δ 8.02 (d, J = 9.2 Hz, 1H), 7.08 – 7.35 (m, 5H), 6.87 (d, J = 2.2 Hz, 1H), 6.63 (dd, J = 2.2, 9.2 Hz, 1H), 3.14 – 3.29 (m, 2H), 2.93 (br. d, J = 11.7 Hz, 2H), 2.54 (d, J = 6.7 Hz, 2H), 2.27 – 2.40 (m, 2H), 1.79 – 2.02 (m, 3H), 1.16 – 1.77 (m, 10H). Anal. calcd for: $C_{24}H_{30}F_3N_3O_2$: C, 64.13; H, 6.73; N, 9.35. Found: C, 64.36; H, 6.72; N, 9.29. LCMS found 449.8, $[M + H]^+$.

N-(5-(6,7-Dimethoxy-3,4-dihydroisoquinolin-2(1H)-yl)pentyl)-4-nitro-3-(trifluoromethyl)aniline (**11b**). The compound has been prepared following procedure C and using 5-((4-nitro-3-(trifluoromethyl)phenyl)amino)pentan-1-ol (**2**) (1.07 mmol, 0.31 g) and 6,7-dimethoxy-1,2,3,4-tetrahydroisoquinoline (2.14 mmol, 0.41 g). The crude product was purified

by flash chromatography eluting 1% MeOH in EtOAc to afford compound **11b** as a yellow solid (yield: 45%). ^{1}H NMR (200 MHz, $CDCl_3$) δ 7.99 (d, *J* = 9.2 Hz, 1H), 6.83 (d, *J* = 2.2 Hz, 1H), 6.50 – 6.62 (m, 3H), 3.81 – 3.90 (m, 6H), 3.59 (s, 2H), 3.16 – 3.32 (m, 2H), 2.68 – 2.90 (m, 4H), 2.56 (t, *J* = 7.3 Hz, 2H), 1.44 – 1.82 (m, 6H). Anal. calcd for: $C_{23}H_{28}F_3N_3O_4$: C, 59.09; H, 6.04; N, 8.99. Found: C, 58.88; H, 6.05; N, 8.93. LCMS found 467.4, $[M + H]^+$.

Radioligand binding assays. In vitro σ_1 ligand binding assays were carried out in Tris-HCl buffer (50 mmol/L, pH 7.4) for 150 min at 37 °C by incubating the guinea pig brain membrane homogenates (500 μg/sample) with [^{3}H]-(+)-Pentazocine (3 nM) and increasing concentrations (from 10^{-5} to 10^{-11} M) of test compound in a final volume of 1 mL. Non-radioactive haloperidol (10 μM) was employed so as to measure non-specific binding. Bound and free radioligand were divided by fast filtration under reduced pressure using a Millipore filter apparatus through GF/B glass fiber filters (Whatman), which were presoaked for 1 h in a 0.5% poly(ethyleneimine) solution. Filters were washed twice with 4 mL of the same ice-cold buffer and the amount of bound radioactivity on the filters air-dried and then soaked in Scintillation cocktail (Ultima Gold MV) was measured using a liquid scintillation counter (Beckman LS6500).[77]

For in vitro the σ_2 binding assays, the membranes (360 μg/sample) were incubated with 3 nM [^{3}H]-1,3-di-o-tolylguanidine ([^{3}H]-DTG) in the presence of the σ_1 masking agent (+)-SKF10,047 (400 nM) at room temperature for 120 min in 0.5 mL (final volume) of binding buffer (50 mmol/L Tris-HCl, pH 8.0). Non-specific binding was evaluated with unlabeled DTG (5 μM). Assays were terminated by adding of ice-cold 10 mM Tris-HCl washing buffer (pH 8.0) and each sample was filtered through Whatman GF/B glass fiber filters, presoaked for 1 h in a 0.5% poly(ethyleneimine) solution. Then, filters were washed with ice-cold buffer (2 × 4 mL) and the amount of bound radioactivity was determined by liquid scintillation counting as described

above.[78] Results are expressed as inhibition constants (K_i values) and calculated using GraphPad Prism (GraphPad Software, San Diego, CA, USA).

NO detection and photolysis experiments. Irradiation of the samples in solution was performed in a thermostated quartz cell (1 cm pathlength, 3 mL capacity) under gentle stirring, by using a continuum laser with λ_{exc} = 405 nm (ca. 100 mW) having a beam diameter of about 1.5 mm. Direct monitoring of NO release for samples in solution was performed by amperometric detection with a World Precision Instrument ISO-NO meter, equipped with a data acquisition system, and based on direct amperometric detection of NO with short response time (< 5 s) and sensitivity range 1 nM – 20 μM. The analog signal was digitalized with a four-channel recording system and transferred to a PC. The sensor was accurately calibrated by mixing standard solutions of $NaNO_2$ with 0.1 M H_2SO_4 and 0.1 M KI according to the reaction:

$$4H^+ + 2I^- + 2NO_2^- \rightarrow 2H_2O + 2NO + I_2$$

Irradiation was performed in a thermostated quartz cell (1 cm pathlength, 3 mL capacity) using the above continuum laser with λ_{exc} = 405 nm. NO measurements were carried out under stirring with the electrode positioned outside the light path in order to avoid NO signal artifacts due to photoelectric interference on the ISO-NO electrode.

NO photogeneration quantum yield (Φ_{NO}) was determined using a continuum laser with λ_{exc} = 405 nm by using following equation:

$$\Phi_{NO} = [NO]\times V / t \times (1\text{-}10^{-A})\times I$$

where [NO] is the concentration of NO, V is the volume of the sample [water:methanol (1:1) solution], t is the irradiation time, A is the absorbance of the sample at the excitation wavelength

and I the intensity of the excitation light source.[79] The I, calculated by potassium ferrioxalate actinometry, was $1.8x10^{14}$ quanta s^{-1}.[79]

Cell culture. The human keratinocyte cell line NCTC-2544 was provided by Interlab Cell Line Collection (Genoa, Italy) and routinely maintained in Minimum Essential Medium (MEM) supplemented with 10% fetal calf serum, 100 U/mL penicillin, and 100 μg/mL streptomycin (Sigma-Aldrich, Milan, Italy). The human melanoma cell line (A2058) and the human breast adenocarcinoma cell line (MCF-7) were obtained from the American Type Culture Collection (Rockville, MD, USA) and were maintained in Dulbecco's modified Eagle's medium (DMEM) containing 10% fetal calf serum, 100 U/mL penicillin, and 100 μg/mL streptomycin (Sigma–Aldrich, Italy). Cell lines were cultured in a humidified atmosphere of 5% CO_2/95% air at 37 °C. Cells from confluent cultures were detached using 0.5% trypsin/0.2% EDTA and seeded in complete medium. Individual wells of a 96-well tissue culture microtiter plate (Falcon; Becton-Dickinson) were inoculated with complete media containing cells in exponential growth at an initial density of $10x10^3$ cells per flat-bottomed well (200 μL per microwell). The plates were incubated at 37 °C in a humidified 5% CO_2 incubator for 24 h before experiments. After medium removal, the drug solutions, previously prepared in DMSO and diluted in culture media, were added to each well and the plates were incubated at 37 °C for 24 h.

Photodynamic activation experiments. Photodynamic activation of compounds was carried out by irradiating all cell lines with a 150 W Xe lamp through a cutoff filter at 390 nm. After 24 h of incubation with the compounds at different concentrations, the supernatant was removed and a phenol red-free medium added to each well. The irradiation time was 15 min. The light effect was evaluated in the untreated cell also.

Cell viability. Cell proliferation was assessed by 3-(4,5-dimethylthiazol-2-yl)-2,5 diphenyltetrazolium bromide (MTT) assay, which is based on the conversion of a substrate containing a tetrazolium ring to the spectrophotometrically detectable formazan by mitochondrial dehydrogenases.[80] Briefly, after treatment of cells with test compounds for 24 h and irradiation, the MTT solution (0.5%, 20 μL) was added to each well. Following incubation at 37°C for 4 h, the supernatant was removed and replaced with 100 μL of DMSO to solubilize formazan crystals. The optical density of each well sample was then measured with a microplate spectrophotometer reader (Digital and Analog Systems, Rome, Italy) at λ=550 nm, and cell viability calculated as percentage respect to each of untreated controls. Each experiment in quadruplicate wells was repeated at least two times and the mean ±SEM for each value was calculated.

Intracellular nitric oxide detection. For intracellular NO detection 2',7'-dichlorofluorescein diacetate (DCF-DA) was used as previously reported.[81,82] For DCF-DA detection, cells were plated in glass cover slips at a density of 50,000 cells and allowed to attach overnight. Cells were serum starved for 24 h and then treated with selected compounds. After 24 h the medium was changed and the cells were incubated with 10 μM DCF-DA for 1 h, washed three times in PBS and irradiated as described above in presence of a phenol red-free medium. For images acquisition, cells were fixed with 4% paraformaldehyde (PFA) in PBS and analyzed under a fluorescence microscope (Axioplan, Zeiss) fitted with 10x and 40x objectives. Images were obtained from random locations on the glass surface and were captured with an MRc5 digital camera (Zeiss).

Total nitrite estimation. Intracellular nitrite content was measured by Griess method as reported by Dubey et al., 2016.[83] After treatments and irradiation, cells were pelleted and lysed with

hypotonic solution. The supernatants were treated with equal volumes of Griess reagent and kept at 37 °C for 30 min in dark.[84] Absorbance was taken at 545 nm and normalized to each sample protein amount that was determined as already reported.[85] Concentration of total nitrite was calculated using sodium nitrite as standard.

AUTHOR INFORMATION

Corresponding Authors

* Prof. Orazio Prezzavento: E-mail, prezzave@unict.it

* Prof. Salvatore Sortino: E-mail: ssortino@unict.it

Author Contributions

The manuscript was written through contributions of all authors. All authors have given approval to the final version of the manuscript.

Notes

The authors declare no competing financial interest.

ACKNOWLEDGMENTS

This work was financially supported by Università degli Studi di Catania, "Piano per la Ricerca 2016–2018 - Linea di Intervento 2 "Dotazione ordinaria" - Code: 57722172105.

ABBREVIATIONS

NO, nitric oxide; NOSs, nitric oxide synthases; RNS, reactive nitrogen species; TLC, thin layer chromatography; TMS, tetramethylsilane; DCF, dichlorofluorescein.

REFERENCES

(1) Chari, R. V. Targeted cancer therapy: conferring specificity to cytotoxic drugs. *Acc. Chem. Res.* **2008**, *41*, 98-107.

(2) Jaracz, S.; Chen, J.; Kuznetsova, L. V.; Ojima, I. Recent advances in tumor-targeting anticancer drug conjugates. *Bioorg. Med. Chem.* **2005**, *13*, 5043-5054.

(3) Srinivasarao, M.; Galliford, C. V.; Low, P. S. Principles in the design of ligand-targeted cancer therapeutics and imaging agents. *Nat. Rev. Drug Discovery* **2015**, *14*, 203-219.

(4) Sievers, E. L.; Senter, P. D. Antibody-drug conjugates in cancer therapy. *Annu. Rev. Med.* **2013**, *64*, 15-29.

(5) Desgrosellier, J. S.; Cheresh, D. A. Integrins in cancer: biological implications and therapeutic opportunities. *Nat. Rev. Cancer* **2010**, *10*, 9-22.

(6) Xia, W.; Low, P. S. Folate-targeted therapies for cancer. *J. Med. Chem.* **2010**, *53*, 6811-6824.

(7) Sortino, S. Photoactivated nanomaterials for biomedical release applications. *J. Mater. Chem.* **2012**, *22*, 301-318.

(8) Dolmans, D. E.; Fukumura, D.; Jain, R. K. Photodynamic therapy for cancer. *Nat. Rev. Cancer* **2003**, *3*, 380-387.

(9) T. Hasan; A. C. E. Moor; Ortel, B. *Cancer Medicine*. 5th ed.; Decker BC Inc. Hamilton, Ontario, Canada: 2000.

(10) Sortino, S. Light-controlled nitric oxide delivering molecular assemblies. *Chem. Soc. Rev.* **2010**, *39*, 2903-2913.

(11) Fry, N. L.; Mascharak, P. K. Photoactive ruthenium nitrosyls as NO donors: how to sensitize them toward visible light. *Acc. Chem. Res.* **2011**, *44*, 289-298.

(12) Ford, P. C. Photochemical delivery of nitric oxide. *Nitric Oxide* **2013**, *34*, 56-64.

(13) Ostrowski, A. D.; Ford, P. C. Metal complexes as photochemical nitric oxide precursors: Potential applications in the treatment of tumors. *Dalton Trans.* **2009**, 10660-10669.

(14) Carpenter, A. W.; Schoenfisch, M. H. Nitric oxide release: Part II. Therapeutic applications. *Chem. Soc. Rev.* **2012**, *41*, 3742-3752.

(15) Ignarro, L. J. *Nitric Oxide: Biology and Pathobiology*. Elsevier Science: Amsterdam, Netherlands, 2000.

(16) Fukumura, D.; Kashiwagi, S.; Jain, R. K. The role of nitric oxide in tumour progression. *Nat. Rev. Cancer* **2006**, *6*, 521-534.

(17) Chang, C. F.; Diers, A. R.; Hogg, N. Cancer cell metabolism and the modulating effects of nitric oxide. *Free Radical Biol. Med.* **2015**, *79*, 324-336.

(18) Guo, M.; Xiang, H. J.; Wang, Y.; Zhang, Q. L.; An, L.; Yang, S. P.; Ma, Y. C.; Wang, Y. C.; Liu, J. G. Ruthenium nitrosyl functionalized graphene quantum dots as an efficient nanoplatform for NIR-light-controlled and mitochondria-targeted delivery of nitric oxide combined with photothermal therapy. *Chem. Commun.* **2017**, *53*, 3253-3256.

(19) Xu, J. S.; Zeng, F.; Wu, H.; Hu, C. P.; Yu, C. M.; Wu, S. Z. Preparation of a mitochondria-targeted and NO-releasing nanoplatform and its enhanced pro-apoptotic effect on cancer cells. *Small* **2014**, *10*, 3750-3760.

(20) Xu, J. S.; Zeng, F.; Wu, H.; Wu, S. Z. A mitochondrial-targeting and NO-based anticancer nanosystem with enhanced photo-controllability and low dark-toxicity. *J. Mater. Chem. B* **2015**, *3*, 4904-4912.

(21) Xiang, H. J.; An, L.; Tang, W. W.; Yang, S. P.; Liu, J. G. Photo-controlled targeted intracellular delivery of both nitric oxide and singlet oxygen using a fluorescence-trackable ruthenium nitrosyl functional nanoplatform. *Chem. Commun.* **2015**, *51*, 2555-2558.

(22) Xiang, H. J.; Guo, M.; An, L.; Yang, S. P.; Zhang, Q. L.; Liu, J. G. A multifunctional nanoplatform for lysosome targeted delivery of nitric oxide and photothermal therapy under 808 nm near-infrared light. *J. Mater. Chem. B* **2016**, *4*, 4667-4674.

(23) Xiang, H. J.; Deng, Q.; An, L.; Guo, M.; Yang, S. P.; Liu, J. G. Tumor cell specific and lysosome-targeted delivery of nitric oxide for enhanced photodynamic therapy triggered by 808 nm near-infrared light. *Chem. Commun.* **2016**, *52*, 148-151.

(24) Kamkaew, A.; Burgess, K. Double-targeting using a TrkC ligand conjugated to dipyrromethene boron difluoride (BODIPY) based photodynamic therapy (PDT) agent. *J. Med. Chem.* **2013**, *56*, 7608-7614.

(25) Spitzer, D.; Simon, P. O., Jr.; Kashiwagi, H.; Xu, J.; Zeng, C.; Vangveravong, S.; Zhou, D.; Chang, K.; McDunn, J. E.; Hornick, J. R.; Goedegebuure, P.; Hotchkiss, R. S.; Mach, R. H.; Hawkins, W. G. Use of multifunctional sigma-2 receptor ligand conjugates to trigger cancer-selective cell death signaling. *Cancer Res.* **2012**, *72*, 201-209.

(26) Kashiwagi, H.; McDunn, J. E.; Simon, P. O., Jr.; Goedegebuure, P. S.; Xu, J.; Jones, L.; Chang, K.; Johnston, F.; Trinkaus, K.; Hotchkiss, R. S.; Mach, R. H.; Hawkins, W. G. Selective sigma-2 ligands preferentially bind to pancreatic adenocarcinomas: applications in diagnostic imaging and therapy. *Mol. Cancer* **2007**, *6*, 48.

(27) Pasquinucci, L.; Prezzavento, O.; Marrazzo, A.; Amata, E.; Ronsisvalle, S.; Georgoussi, Z.; Fourla, D. D.; Scoto, G. M.; Parenti, C.; Arico, G.; Ronsisvalle, G. Evaluation of *N*-substitution in 6,7-benzomorphan compounds. *Bioorg. Med. Chem.* **2010**, *18*, 4975-4982.

(28) Parenti, C.; Turnaturi, R.; Arico, G.; Marrazzo, A.; Prezzavento, O.; Ronsisvalle, S.; Scoto, G. M.; Ronsisvalle, G.; Pasquinucci, L. Antinociceptive profile of LP1, a non-peptide multitarget opioid ligand. *Life Sci.* **2012**, *90*, 957-961.

(29) Prezzavento, O.; Campisi, A.; Parenti, C.; Ronsisvalle, S.; Arico, G.; Arena, E.; Pistolozzi, M.; Scoto, G. M.; Bertucci, C.; Vanella, A.; Ronsisvalle, G. Synthesis and resolution of cis-(+/-)-methyl (1R,2S/1S,2R)-2-[(4-hydroxy-4-phenylpiperidin-1-yl)methyl]-1-(4-methylphenyl)cycl opropanecarboxylate [(+/-)-PPCC)]: new sigma receptor ligands with neuroprotective effect. *J. Med. Chem.* **2010**, *53*, 5881-5885.

(30) Hayashi, T.; Su, T. P. Sigma-1 receptor chaperones at the ER-mitochondrion interface regulate Ca(2+) signaling and cell survival. *Cell* **2007**, *131*, 596-610.

(31) Su, T. P.; Hayashi, T.; Maurice, T.; Buch, S.; Ruoho, A. E. The sigma-1 receptor chaperone as an inter-organelle signaling modulator. *Trends Pharmacol. Sci.* **2010**, *31*, 557-566.

(32) Schmidt, H. R.; Zheng, S.; Gurpinar, E.; Koehl, A.; Manglik, A.; Kruse, A. C. Crystal structure of the human sigma1 receptor. *Nature* **2016**, *532*, 527-530.

(33) Prezzavento, O.; Arena, E.; Parenti, C.; Pasquinucci, L.; Arico, G.; Scoto, G. M.; Grancara, S.; Toninello, A.; Ronsisvalle, S. Design and synthesis of new bifunctional sigma-1 selective ligands with antioxidant activity. *J. Med. Chem.* **2013**, *56*, 2447-2455.

(34) Maurice, T. Improving Alzheimer's disease-related cognitive deficits with sigma-1 receptor Agonists. *Drug News Perspect.* **2002**, *15*, 617-625.

(35) Chu, U. B.; Ruoho, A. E. Biochemical pharmacology of the sigma-1 receptor. *Mol. Pharmacol.* **2016**, *89*, 142-153.

(36) Prezzavento, O.; Arena, E.; Sanchez-Fernandez, C.; Turnaturi, R.; Parenti, C.; Marrazzo, A.; Catalano, R.; Amata, E.; Pasquinucci, L.; Cobos, E. J. (+)-and (-)-phenazocine enantiomers:

evaluation of their dual opioid agonist/sigma1 antagonist properties and antinociceptive effects. *Eur. J. Med. Chem.* **2017**, *125*, 603-610.

(37) Olivieri, M.; Amata, E.; Vinciguerra, S.; Fiorito, J.; Giurdanella, G.; Drago, F.; Caporarello, N.; Prezzavento, O.; Arena, E.; Salerno, L.; Rescifina, A.; Lupo, G.; Anfuso, C. D.; Marrazzo, A. Antiangiogenic effect of (+/-)-haloperidol metabolite II valproate ester [(+/-)-MRJF22] in human microvascular retinal endothelial cells. *J. Med. Chem.* **2016**, *59*, 9960-9966.

(38) Mesangeau, C.; Amata, E.; Alsharif, W.; Seminerio, M. J.; Robson, M. J.; Matsumoto, R. R.; Poupaert, J. H.; McCurdy, C. R. Synthesis and pharmacological evaluation of indole-based sigma receptor ligands. *Eur. J. Med. Chem.* **2011**, *46*, 5154-5161.

(39) Marrazzo, A.; Fiorito, J.; Zappala, L.; Prezzavento, O.; Ronsisvalle, S.; Pasquinucci, L.; Scoto, G. M.; Bernardini, R.; Ronsisvalle, G. Antiproliferative activity of phenylbutyrate ester of haloperidol metabolite II [(+/-)-MRJF4] in prostate cancer cells. *Eur. J. Med. Chem.* **2011**, *46*, 433-438.

(40) Parenti, C.; Marrazzo, A.; Arico, G.; Parenti, R.; Pasquinucci, L.; Ronsisvalle, S.; Ronsisvalle, G.; Scoto, G. M. The antagonistic effect of the sigma 1 receptor ligand (+)-MR200 on persistent pain induced by inflammation. *Inflammation Res.* **2014**, *63*, 231-237.

(41) Crottes, D.; Guizouarn, H.; Martin, P.; Borgese, F.; Soriani, O. The sigma-1 receptor: a regulator of cancer cell electrical plasticity? *Front. Physiol.* **2013**, *4*, 175.

(42) Aydar, E.; Onganer, P.; Perrett, R.; Djamgoz, M. B.; Palmer, C. P. The expression and functional characterization of sigma (sigma) 1 receptors in breast cancer cell lines. *Cancer Lett.* **2006**, *242*, 245-257.

(43) Alon, A.; Schmidt, H. R.; Wood, M. D.; Sahn, J. J.; Martin, S. F.; Kruse, A. C. Identification of the gene that codes for the sigma2 receptor. *Proc. Natl. Acad. Sci. U. S. A.* **2017**, *114*, 7160-7165.

(44) Geldenhuys, W. J.; Novotny, N.; Malan, S. F.; Van der Schyf, C. J. 3D-QSAR and docking studies of pentacycloundecylamines at the sigma-1 (sigma1) receptor. *Bioorg. Med. Chem. Lett.* **2013**, *23*, 1707-1711.

(45) Rescifina, A.; Floresta, G.; Marrazzo, A.; Parenti, C.; Prezzavento, O.; Nastasi, G.; Dichiara, M.; Amata, E. Development of a sigma-2 receptor affinity filter through a monte carlo based QSAR analysis. *Eur. J. Pharm. Sci.* **2017**, *106*, 94-101.

(46) Rescifina, A.; Floresta, G.; Marrazzo, A.; Parenti, C.; Prezzavento, O.; Nastasi, G.; Dichiara, M.; Amata, E. Sigma-2 receptor ligands QSAR model dataset. *Data in Brief* **2017**, *13*, 514-535.

(47) Nastasi, G.; Miceli, C.; Pittala, V.; Modica, M. N.; Prezzavento, O.; Romeo, G.; Rescifina, A.; Marrazzo, A.; Amata, E. S2RSLDB: a comprehensive manually curated, internet-accessible database of the sigma-2 receptor selective ligands. *J. Cheminf.* **2017**, *9*, 1-9.

(48) Chu, U. B.; Mavlyutov, T. A.; Chu, M. L.; Yang, H.; Schulman, A.; Mesangeau, C.; McCurdy, C. R.; Guo, L. W.; Ruoho, A. E. The sigma-2 receptor and progesterone receptor membrane component 1 are different binding sites derived from independent genes. *EBioMedicine* **2015**, *2*, 1806-1813.

(49) Mach, R. H.; Zeng, C.; Hawkins, W. G. The sigma2 receptor: a novel protein for the imaging and treatment of cancer. *J. Med. Chem.* **2013**, *56*, 7137-7160.

(50) van Waarde, A.; Rybczynska, A. A.; Ramakrishnan, N.; Ishiwata, K.; Elsinga, P. H.; Dierckx, R. A. Sigma receptors in oncology: therapeutic and diagnostic applications of sigma ligands. *Curr. Pharm. Des.* **2010**, *16*, 3519-3537.

(51) Xu, J.; Zeng, C.; Chu, W.; Pan, F.; Rothfuss, J. M.; Zhang, F.; Tu, Z.; Zhou, D.; Zeng, D.; Vangveravong, S.; Johnston, F.; Spitzer, D.; Chang, K. C.; Hotchkiss, R. S.; Hawkins, W. G.; Wheeler, K. T.; Mach, R. H. Identification of the PGRMC1 protein complex as the putative sigma-2 receptor binding site. *Nat. Commun.* **2011**, *2*, 380.

(52) Washington University School of Medicine. [^{18}F]ISO-1 PET/CT in breast cancer. In: ClinicalTrials.gov. Available from: https://clinicaltrials.gov/ct2/show/NCT02284919. NLM Identifier: NCT02284919. Oct 8, 2017.

(53) Washington University School of Medicine. Assessment of cellular proliferation in tumors by positron emission tomography (PET) using [^{18}F]ISO-1 (FISO PET/CT). In: ClinicalTrials.gov. Available from: https://clinicaltrials.gov/ct2/show/NCT00968656. NLM Identifier: NCT00968656. Oct 8, 2017.

(54) Abramson Cancer Center of the University of Pennsylvania. Imaging of in vivo sigma-2 receptor expression with ^{18}F-ISO-1 positron emission tomography in metastatic breast cancer. In: ClinicalTrials.gov. Available from: https://clinicaltrials.gov/ct2/show/NCT03057743. NLM Identifier: NCT03057743. Oct 8, 2017.

(55) van Waarde, A.; Rybczynska, A. A.; Ramakrishnan, N. K.; Ishiwata, K.; Elsinga, P. H.; Dierckx, R. A. Potential applications for sigma receptor ligands in cancer diagnosis and therapy. *Biochim. Biophys. Acta* **2015**, *1848*, 2703-2714.

(56) Fitzgerald, K. A.; Malhotra, M.; Gooding, M.; Sallas, F.; Evans, J. C.; Darcy, R.; O'Driscoll, C. M. A novel, anisamide-targeted cyclodextrin nanoformulation for siRNA delivery to prostate cancer cells expressing the sigma-1 receptor. *Int. J. Pharm.* **2016**, *499*, 131-145.

(57) Zhang, Y.; Huang, Y.; Zhang, P.; Gao, X.; Gibbs, R. B.; Li, S. Incorporation of a selective sigma-2 receptor ligand enhances uptake of liposomes by multiple cancer cells. *Int. J. Nanomed.* **2012**, *7*, 4473-4485.

(58) Schinina, B.; Martorana, A.; Colabufo, N. A.; Contino, M.; Niso, M.; Perrone, M. G.; De Guidi, G.; Catalfo, A.; Rappazzo, G.; Zuccarello, E.; Prezzavento, O.; Amata, E.; Rescifina, A.; Marrazzo, A. 4-Nitro-2,1,3-benzoxadiazole derivatives as potential fluorescent sigma receptor probes. *RSC Adv.* **2015**, *5*, 47108-47116.

(59) Ronsisvalle, S.; Arico, G.; Cova, A. M.; Blanco, P.; Amata, E.; Pappalardo, M.; Pasquinucci, L.; Spadaro, A.; Ronsisvalle, N. Caspase-3 activation in human melanoma A375 cell line by a novel selective sigma-2 agonist. *Pharmazie* **2016**, *71*, 146-151.

(60) Fraix, A.; Marino, N.; Sortino, S. Phototherapeutic release of nitric oxide with engineered nanoconstructs. *Top. Curr. Chem.* **2016**, *370*, 225-257.

(61) Fraix, A.; Sortino, S. Photoactivable platforms for nitric oxide delivery with fluorescence imaging. *Chem. - Asian J.* **2015**, *10*, 1116-1125.

(62) Caruso, E. B.; Petralia, S.; Conoci, S.; Giuffrida, S.; Sortino, S. Photodelivery of nitric oxide from water-soluble platinum nanoparticles. *J. Am. Chem. Soc.* **2007**, *129*, 480-481.

(63) Fraix, A.; Kandoth, N.; Manet, I.; Cardile, V.; Graziano, A. C. E.; Gref, R.; Sortino, S. An engineered nanoplatform for bimodal anticancer phototherapy with dual-color fluorescence detection of sensitizers. *Chem. Commun.* **2013**, *49*, 4459-4461.

(64) Fraix, A.; Blangetti, M.; Guglielmo, S.; Lazzarato, L.; Marino, N.; Cardile, V.; Graziano, A. C. E.; Manet, I.; Fruttero, R.; Gasco, A.; Sortino, S. Light-tunable generation of singlet oxygen and nitric oxide with a bichromophoric molecular hybrid: a bimodal approach to killing cancer cells. *ChemMedChem* **2016**, *11*, 1371-1379.

(65) Fowley, C.; McHale, A. P.; McCaughan, B.; Fraix, A.; Sortino, S.; Callan, J. F. Carbon quantum dot-NO photoreleaser nanohybrids for two-photon phototherapy of hypoxic tumors. *Chem. Commun.* **2015**, *51*, 81-84.

(66) Chegaev, K.; Fraix, A.; Gazzano, E.; Abd-Ellatef, G. E. F.; Blangetti, M.; Rolando, B.; Conoci, S.; Riganti, C.; Fruttero, R.; Gasco, A.; Sortino, S. Light-regulated NO release as a novel strategy to overcome doxorubicin multidrug resistance. *ACS Med. Chem. Lett.* **2017**, *8*, 361-365.

(67) Navacchia, M. L.; Fraix, A.; Chinaglia, N.; Gallerani, E.; Perrone, D.; Cardile, V.; Graziano, A. C. E.; Capobianco, M. L.; Sortino, S. NO photoreleaser-deoxyadenosine and -bile acid derivative bioconjugates as novel potential photochemotherapeutics. *ACS Med. Chem. Lett.* **2016**, *7*, 939-943.

(68) Mach, R. H.; Smith, C. R.; al-Nabulsi, I.; Whirrett, B. R.; Childers, S. R.; Wheeler, K. T. Sigma 2 receptors as potential biomarkers of proliferation in breast cancer. *Cancer Res.* **1997**, *57*, 156-161.

(69) Gitto, R.; De Luca, L.; Ferro, S.; Scala, A.; Ronsisvalle, S.; Parenti, C.; Prezzavento, O.; Buemi, M. R.; Chimirri, A. From NMDA receptor antagonists to discovery of selective sigma(2) receptor ligands. *Bioorg. Med. Chem.* **2014**, *22*, 393-397.

(70) Amata, E.; Bland, N. D.; Campbell, R. K.; Pollastri, M. P. Evaluation of pyrrolidine and pyrazolone derivatives as inhibitors of trypanosomal phosphodiesterase B1 (TbrPDEB1). *Tetrahedron Lett.* **2015**, *56*, 2832-2835.

(71) Amata, E.; Bland, N. D.; Hoyt, C. T.; Settimo, L.; Campbell, R. K.; Pollastri, M. P. Repurposing human PDE4 inhibitors for neglected tropical diseases: Design, synthesis and evaluation of cilomilast analogues as trypanosoma brucei PDEB1 inhibitors. *Bioorg. Med. Chem. Lett.* **2014**, *24*, 4084-4089.

(72) Romeo, R.; Carnovale, C.; Giofre, S. V.; Chiacchio, M. A.; Garozzo, A.; Amata, E.; Romeo, G.; Chiacchio, U. C-5'-Triazolyl-2'-oxa-3'-aza-4'a-carbanucleosides: Synthesis and biological evaluation. *Beilstein J. Org. Chem.* **2015**, *11*, 328-334.

(73) Devine, W.; Woodring, J. L.; Swaminathan, U.; Amata, E.; Patel, G.; Erath, J.; Roncal, N. E.; Lee, P. J.; Leed, S. E.; Rodriguez, A.; Mensa-Wilmot, K.; Sciotti, R. J.; Pollastri, M. P. Protozoan parasite growth inhibitors discovered by cross-screening yield potent scaffolds for lead discovery. *J. Med. Chem.* **2015**, *58*, 5522-5537.

(74) Callari, F. L.; Sortino, S. Amplified nitric oxide photorelease in DNA proximity. *Chem. Commun.* **2008**, *17*, 1971-1973.

(75) Vilner, B. J.; John, C. S.; Bowen, W. D. Sigma-1 and sigma-2 receptors are expressed in a wide variety of human and rodent tumor-cell lines. *Cancer Res.* **1995**, *55*, 408-413.

(76) John, C. S.; Bowen, W. D.; Saga, T.; Kinuya, S.; Vilner, B. J.; Baumgold, J.; Paik, C. H.; Reba, R. C.; Neumann, R. D.; Varma, V. M.; et al. A malignant melanoma imaging agent: synthesis, characterization, in vitro binding and biodistribution of iodine-125-(2-piperidinylaminoethyl)4-iodobenzamide. *J. Nucl. Med.* **1993**, *34*, 2169-2175.

(77) DeHaven-Hudkins, D. L.; Fleissner, L. C.; Ford-Rice, F. Y. Characterization of the binding of [3H](+)-pentazocine to sigma recognition sites in guinea pig brain. *Eur. J. Pharmacol.* **1992**, *227*, 371-378.

(78) Mach, R. H.; Smith, C. R.; Childers, S. R. Ibogaine possesses a selective affinity for sigma 2 receptors. *Life Sci.* **1995**, *57*, Pl57-62.

(79) Montalti, M.; Credi, A.; Prodi, L.; Gandolfi, M. T. *Handbook of Photochemistry*. 3rd ed.; CRC Press. Boca Raton, Florida: 2006.

(80) Graziano, A. C. E.; Parenti, R.; Avola, R.; Cardile, V. Krabbe disease: involvement of connexin43 in the apoptotic effects of sphingolipid psychosine on mouse oligodendrocyte precursors. *Apoptosis* **2016**, *21*, 25-35.

(81) Gunasekar, P. G.; Kanthasamy, A. G.; Borowitz, J. L.; Isom, G. E. Monitoring intracellular nitric oxide formation by dichlorofluorescin in neuronal cells. *J. Neurosci. Methods* **1995**, *61*, 15-21.

(82) Kasim, N.; Branton, R. L.; Clarke, D. J. Neuronal nitric oxide synthase immunohistochemistry and 4,5-diaminofluorescein diacetate: tools for nitric oxide research. *J. Neurosci. Methods* **2001**, *112*, 1-8.

(83) Dubey, M.; Nagarkoti, S.; Awasthi, D.; Singh, A. K.; Chandra, T.; Kumaravelu, J.; Barthwal, M. K.; Dikshit, M. Nitric oxide-mediated apoptosis of neutrophils through caspase-8 and caspase-3-dependent mechanism. *Cell Death Dis.* **2016**, *7*.

(84) Graziano, A. C. E.; Cardile, V.; Crasci, L.; Caggia, S.; Dugo, P.; Bonina, F.; Panico, A. Protective effects of an extract from Citrus bergamia against inflammatory injury in interferon-gamma and histamine exposed human keratinocytes. *Life Sci.* **2012**, *90*, 968-974.

(85) Graziano, A. C. E.; Avola, R.; Pannuzzo, G.; Cardile, V. Aquaporin1 and 3 modification as a result of chondrogenic differentiation of human mesenchymal stem cell. *J. Cell. Physiol.* [Online early access]. DOI: 10.1002/jcp.26100. Published Online: Aug 28, 2017. http://onlinelibrary.wiley.com/doi/10.1002/jcp.26100/abstract (accessed Nov 21, 2017).

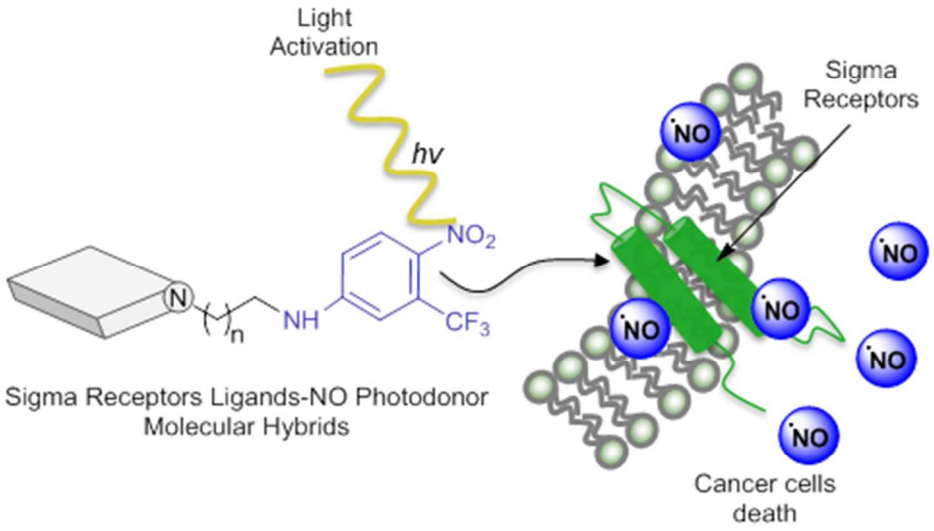

Table of contents graphic

43x24mm (300 x 300 DPI)

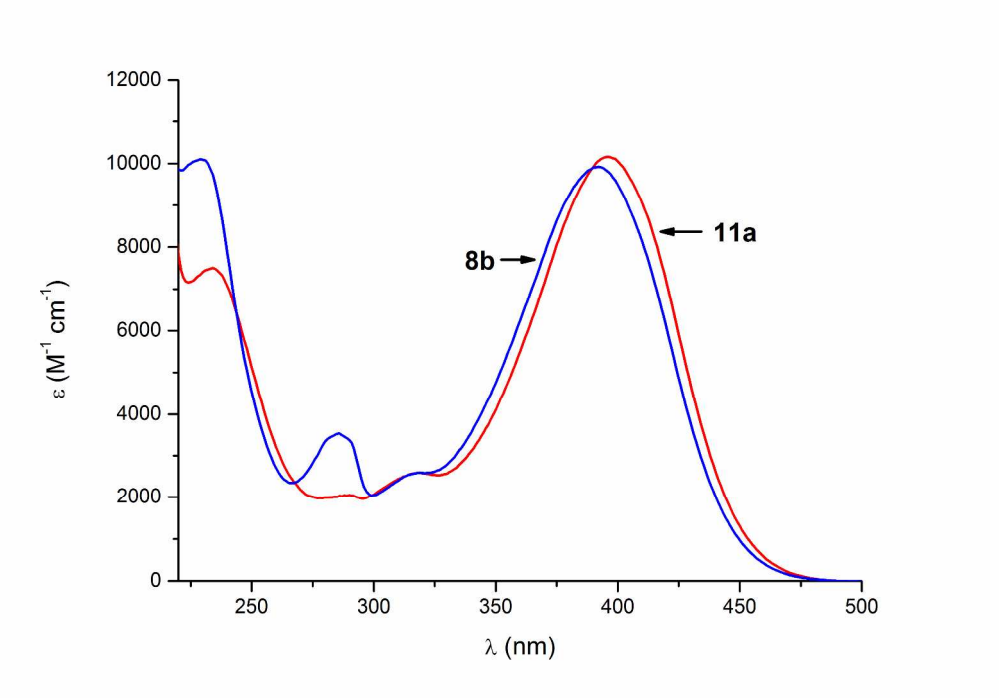

Figure 2. Absorption spectra of 8a and 11a in water:methanol (1:1)

288x201mm (300 x 300 DPI)

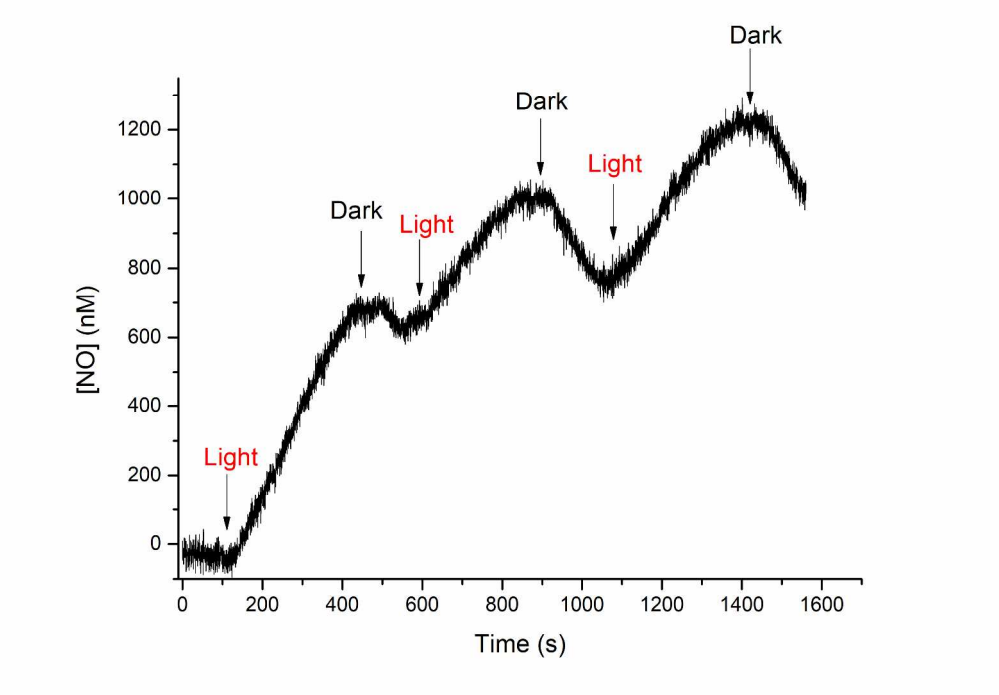

Figure 3. NO release profiles observed upon visible light irradiation (λexc = 405 nm) of a water:methanol (1:1) solution of 11b (50 μM).

288x201mm (300 x 300 DPI)

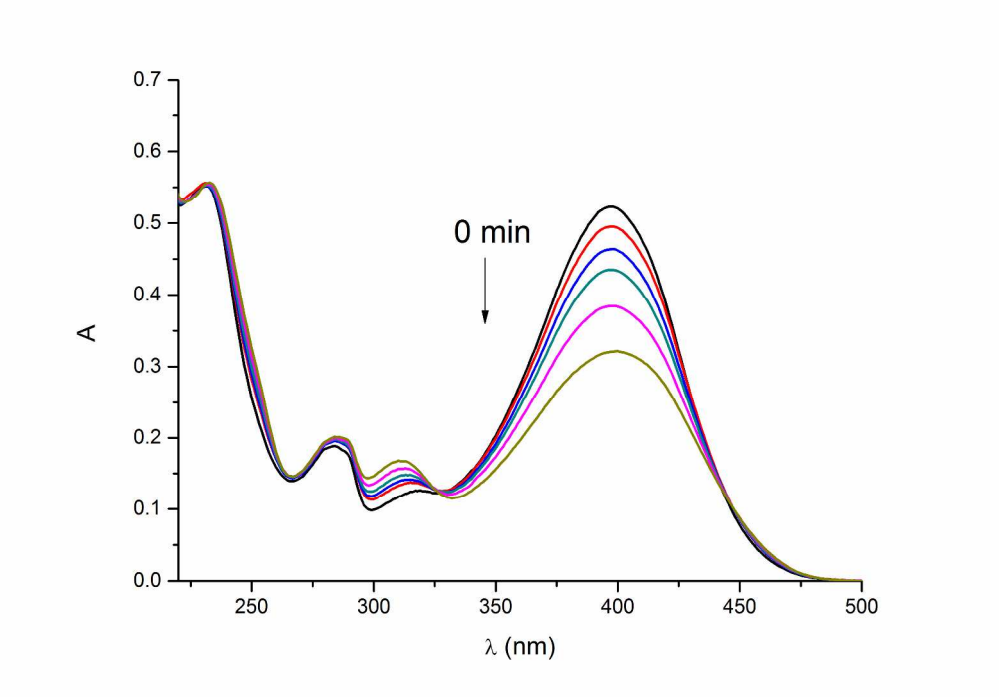

Figure 4. Absorption spectral changes observed upon visible light irradiation (λexc = 405 nm) of a water:methanol (1:1) solution of 11b (50 μM) from 0 to 85 min.

288x201mm (300 x 300 DPI)

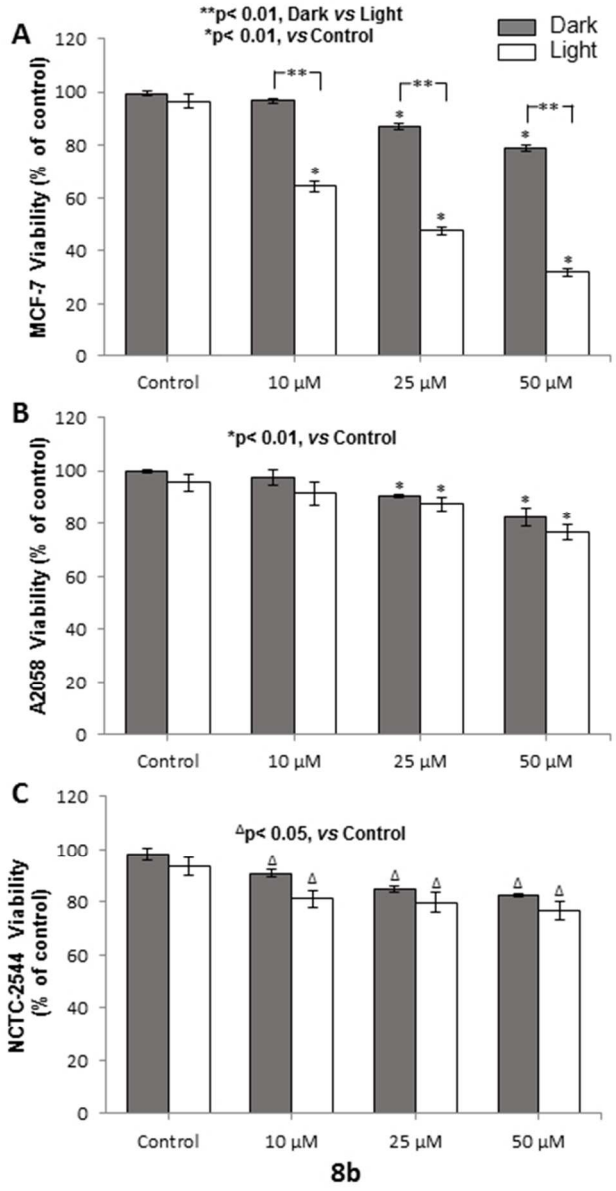

Figure 5. Photodynamic activation of compound 8b. Various concentrations of compound 8b were added to MCF-7 (Panel A), A2058 (Panel B), and NCTC-2544 (Panel C) cell lines for 24 hours. Cytotoxicity was determined by MTT assay both in dark condition and after 15 min irradiation. Results are expressed as percentage of cell viability. Each data point represents the mean of quadruplicate samplings from 96-well microplates ± SD.

34x66mm (300 x 300 DPI)

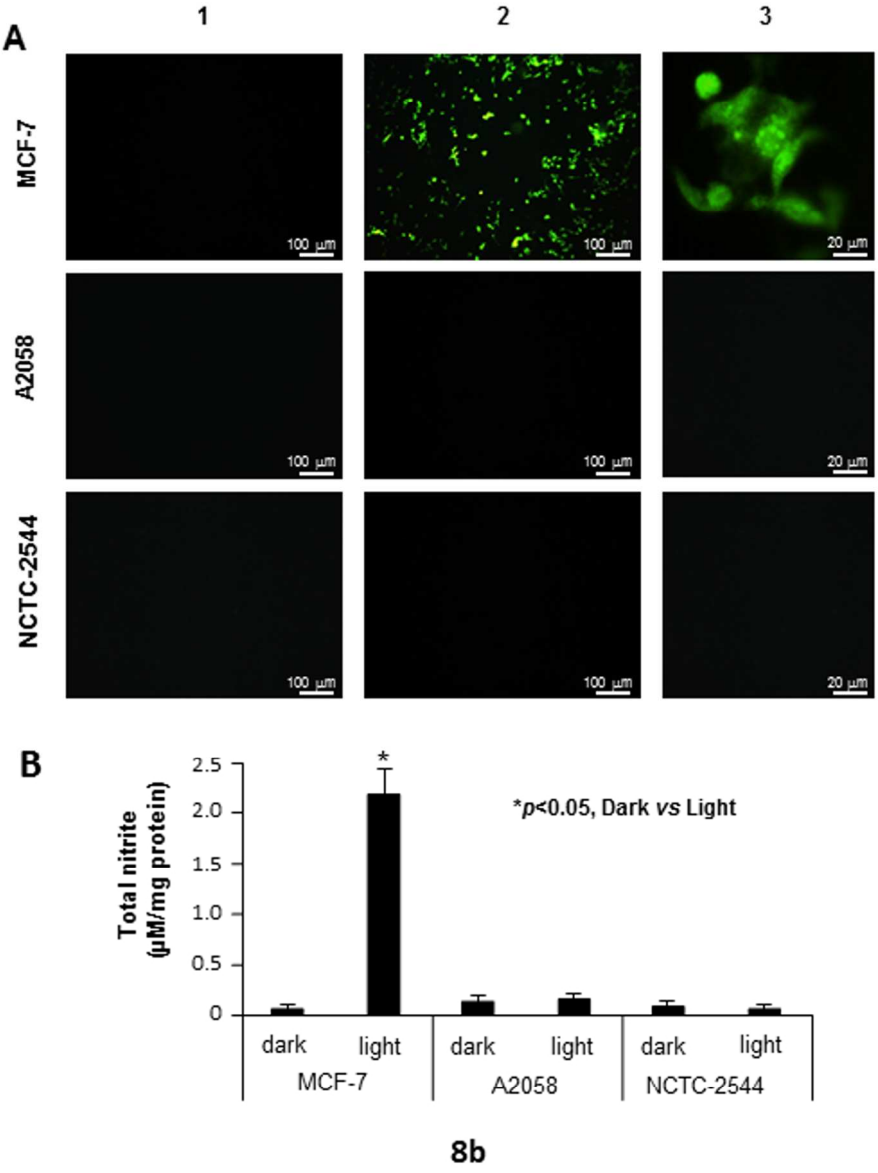

Figure 6. Intracellular NO detection and total nitrite estimation for compound 8b. (Panel A) Intracellular NO evaluation in cell lines exposed to 50 µM of 8b determined by DCF-DA and visualized by fluorescence microscopy. Line 1: dark (10x); line 2: light-treated cells (10x); line 3: light-treated cells (40x). (Panel B) Total nitrite content measured using Griess reagent in cells treated with compound 8b (50 µM) under dark (control) or light conditions.

102x135mm (300 x 300 DPI)

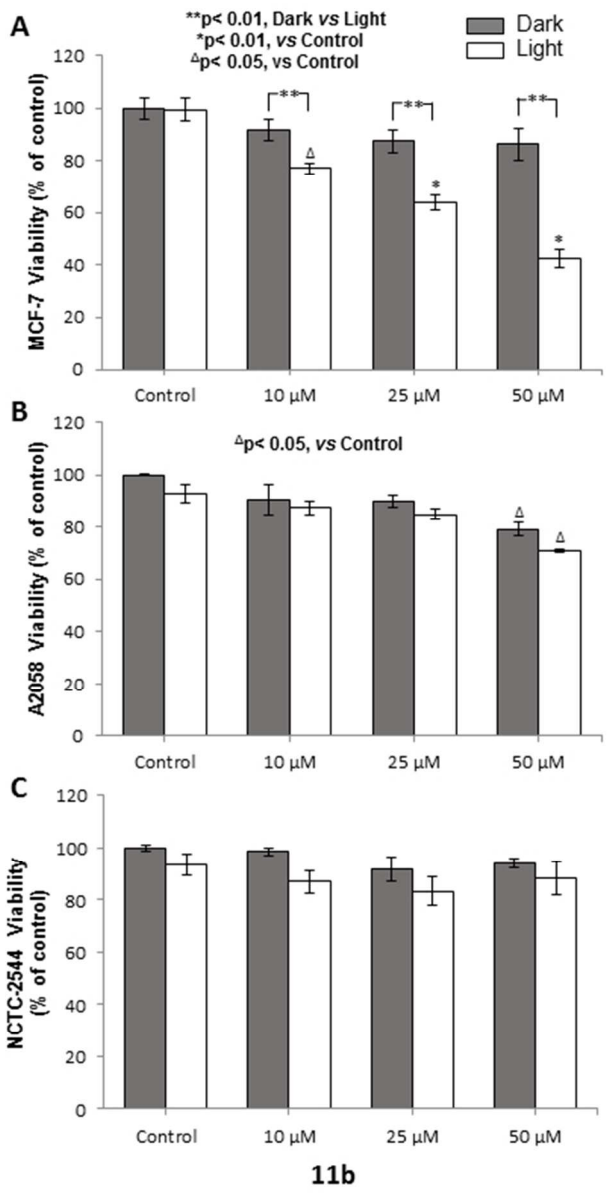

Figure 7. Photodynamic activation of compound 11b. Various concentrations of compound 11b were added to MCF-7 (Panel A), A2058 (Panel B), and NCTC-2544 (Panel C) cell lines for 24 hours. Cytotoxicity was determined by MTT assay both in dark condition and after 15 min irradiation. Results are expressed as the percentage of cell viability. Each data point represents the mean of quadruplicate samplings from 96-well microplates ± SD.

34x67mm (300 x 300 DPI)

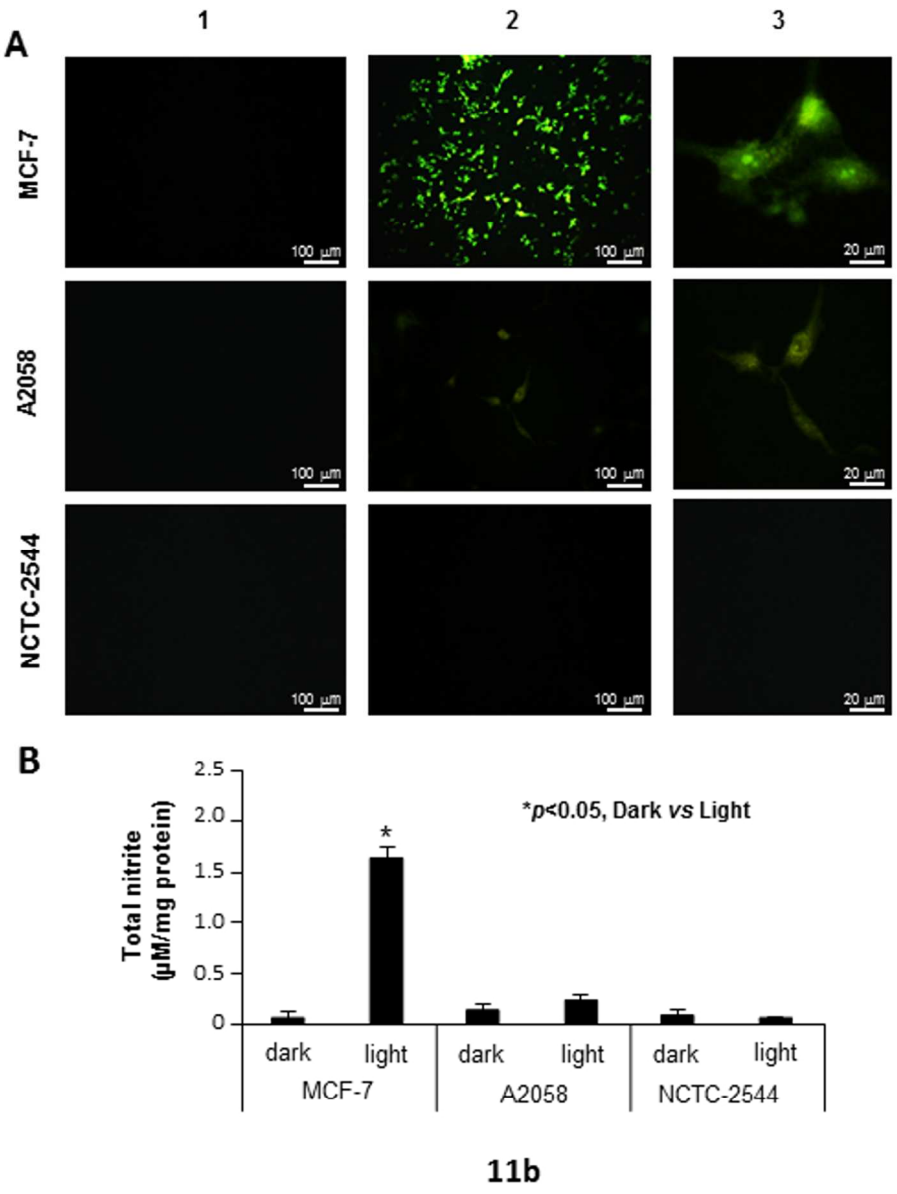

11b

Figure 8. Intracellular NO detection and total nitrite estimation for compound 11b. (Panel A) Intracellular NO evaluation in cell lines exposed to 50 µM of 11b determined by DCF-DA and visualized by fluorescence microscopy. Line 1: dark (10x); line 2: light-treated cells (10x); line 3: light-treated cells (40x). (Panel B) Total nitrite content measured using Griess reagent in cells treated with compound 11b (50 µM) under dark (control) or light conditions.

102x135mm (300 x 300 DPI)

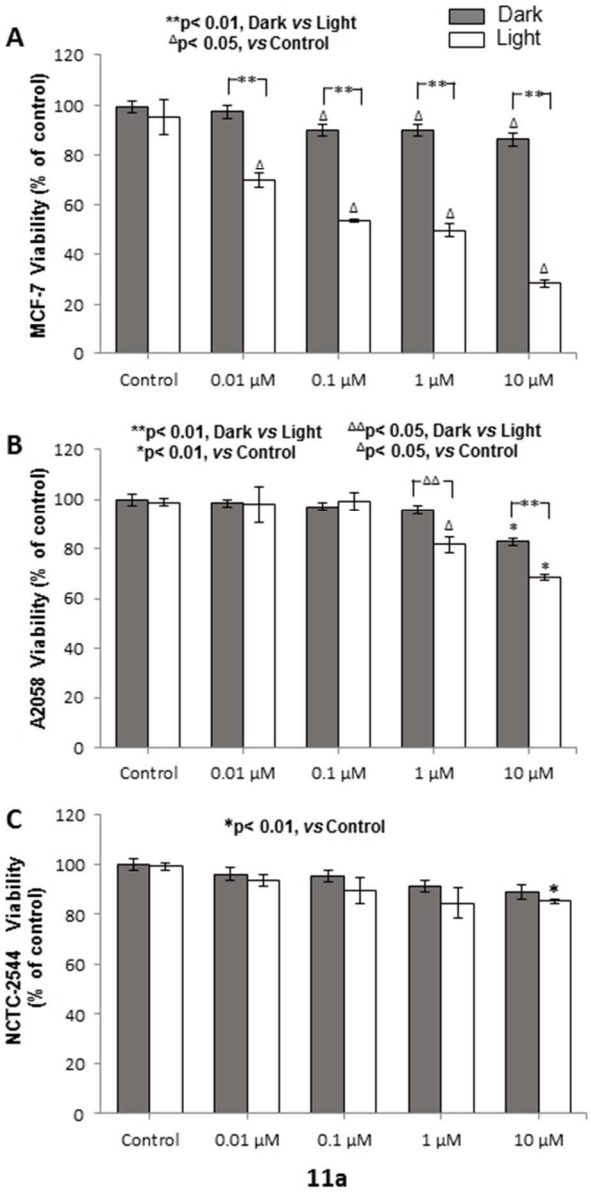

11a

Figure 9. Photodynamic activation of compound 11a. Various concentrations of compound 11a were added to MCF-7 (Panel A), A2058 (Panel B), and NCTC-2544 (Panel C) cell lines for 24 hours. Cytotoxicity was determined by MTT assay both in dark condition and after 15 min irradiation. Results are expressed as the percentage of cell viability. Each data point represents the mean of quadruplicate samplings from 96-well microplates ± SD.

35x70mm (300 x 300 DPI)

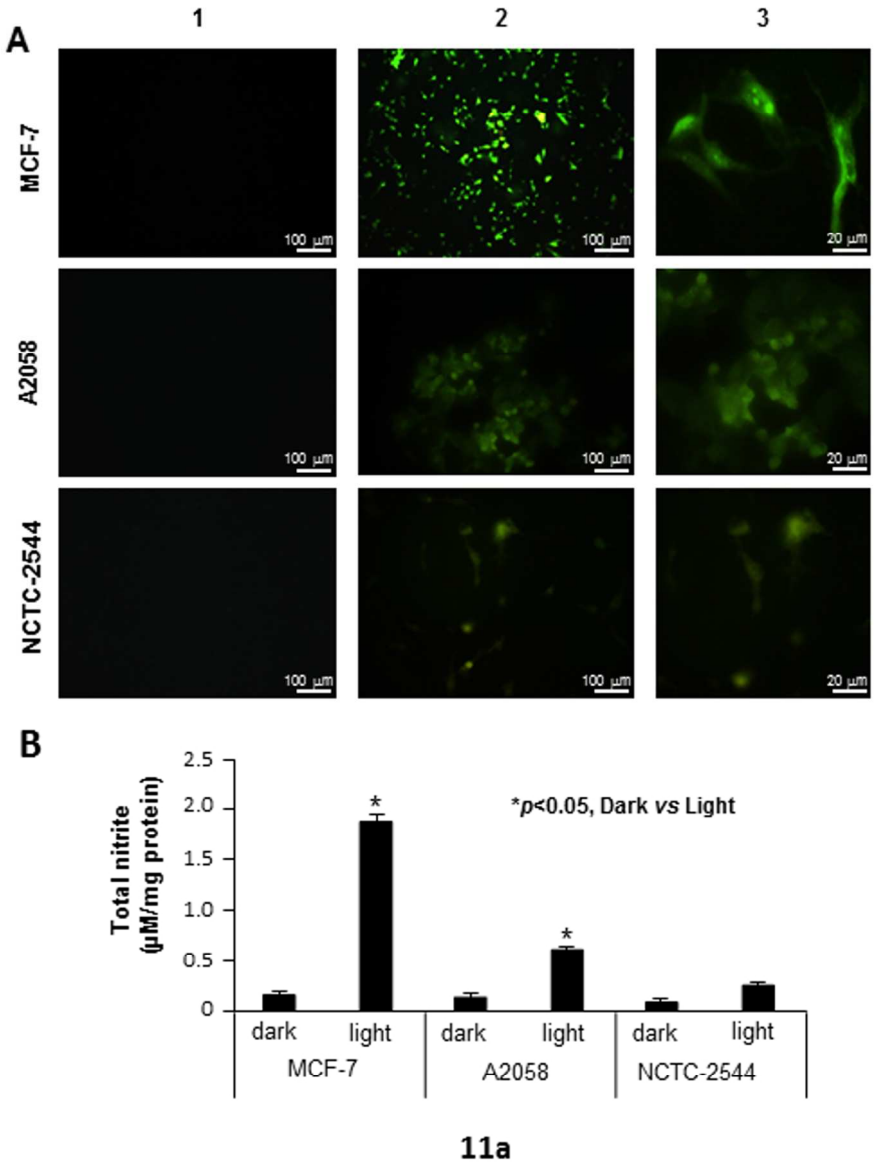

Figure 10. Intracellular NO detection and total nitrite estimation for compound 11a. (Panel A) Intracellular NO evaluation in cell lines exposed to 10 µM of 11a determined by DCF-DA and visualized by fluorescence microscopy. Line 1: dark (10x); line 2: light-treated cells (10x); line 3: light-treated cells (40x). (Panel B) Total nitrite content measured using Griess reagent in cells treated with compound 11a (10 µM) under dark (control) or light conditions.

100x135mm (300 x 300 DPI)